Contraction Fronts Of The Left Cardiac Ventricle

A Case For High Frame Rate Ultrasound

Vandborg Andersen, Martin

Publication date:
2019

Document Version
Publisher's PDF, also known as Version of record

CONTRACTION FRONTS OF THE LEFT CARDIAC VENTRICLE

A CASE FOR HIGH FRAME RATE ULTRASOUND

BY
MARTIN SIEMIENSKI ANDERSEN

DISSERTATION SUBMITTED 2019

AALBORG UNIVERSITY
DENMARK

Contraction Fronts Of The Left Cardiac Ventricle: A Case For High Frame Rate Ultrasound

Ph.D. Dissertation

Martin Siemienski Andersen

Dissertation submitted month 09, 2019

Dissertation submitted: August, 2019

PhD supervisors: Associate Prof. Samuel E. Schmidt, PhD, MSc
Aalborg University

Professor Johannes J. Struijk, PhD, MSc
Aalborg University

External Supervisors: Professor Olaf T. von Ramm, PhD, MSc
Duke University

Professor Joseph Kisslo, MD
Duke University Hospital

Professor Peter Søgaard, MD
Aalborg University Hospital

PhD committee: Associate Professor, PhD Dan S. Karbing
Aalborg University

Professor, PhD Jan D'hooge
Katholieke Universiteit Leuven

Professor, Dr.med. Asbjørn Støylen
Norwegian University of Science and Technology

PhD Series: Faculty of Medicine, Aalborg University

Department: Department of Health Science and Technology

ISSN (online): 2246-1302
ISBN (online): 978-87-7210-476-8

Published by:
Aalborg University Press
Langagervej 2
DK – 9220 Aalborg Ø
Phone: +45 99407140
aauf@forlag.aau.dk
forlag.aau.dk

Printed in Denmark by Rosendahls, 2019

Curriculum Vitae

Martin Siemienski Andersen

Martin's current research field is high-frame-rate echocardiographic image analysis. In 2015, he received his Master's in biomedical engineering from Aalborg University in Denmark. He was the recipient of the Fulbright Scholarship in 2016 to work on a "High-Speed Strain Determination" project with the von Ramm laboratory at Duke University's Pratt School of Engineering and Duke University Hospital. During the Fall of 2018, he attended the Business Accelerated Academy at the BioInnovative Institute in Copenhagen for business development for what would later be called HeartView Medical. As of 2019 he works as a Ph.D. Fellow and Research assistant at Aalborg University on the "Cardiac Excitation Contraction Coupling" project, where his research interests revolved around electromechanical coupling to better understand the transient mechanical waves within the human heart. These interests are linked to his goal to better patient outcomes by improving the quality of information from diagnostic imaging.

Curriculum Vitae

Abstract

Introduction: This dissertation sought to find a methodology for visualization and quantification of the propagation of mechanical fronts through the Left Ventricle (LV).

Methods: Duke University's T5 ultrasound system was used for image acquisition. The T5 is an experimental phased array ultrasound system capable of up to 2500 images per second (fps) for some application or 1000 fps for adult cardiac imaging using full field of view while simultaneously showing a live display of the images. The validation image sequences were generated using a high precision translation stage capable of horizontal and vertical motion at 10 μm increments and a tissue mimicking phantom. The second type of images were high frame rate (HFR) in vivo cardiac images with frame rates between 300 fps and 1000 fps.

Results: Studies A and B presented the Continuous Feature-Tracking (CFT) algorithm, which was capable of accurately describing kinematics. Study C was the first study to show a statistically significant mechanical propagation origin for patients with echocardiographic normal LV function: The mid septal wall segment. These identified fronts were consistently moving faster than the electrical excitation velocity through the electrical pathways of the Left Bundle Branch (LBB) and Purkinje network. A new visualization method using strain rate called a Strain Rate Image (SRI) was developed. The strain rate emphasized changes in the myocardial deformation while presenting them as an image, which made visual interpretation of contraction propagation possible. Study D found statistical significant differences in the duration of the transient fronts associated with tissue shortening between patients with echocardiographic normal LV function, Left Bundle Branch Block (LBBB), and non-LBBB conduction disorder. Furthermore, a new method using a modified correlation coefficient was developed, which in turn illustrated significantly different measurements when comparing patient groups.

Conclusion: It was possible to extract propagating mechanical fronts from HFR B-mode echocardiographic images. Differences of transient mechanical events between different patient groups were identified. Finally, it was shown how strain should be used in conjunction with HFR echocardiographic images when identifying short-transient and rapidly propagating mechanical contractile fronts.

Abstract

Resumé

Introduktion: Denne afhandling søgte at finde en metode til visualisering og kvantificering af udbredelsen af mekaniske kontraktion fronter gennem den venstre ventrikel (LV).

Metode: Duke University's T5 ultralyds systemet blev brugt til billede optagelse. T5 systemet er et eksperimentelt fase-array ultralydssystem som kan optage billeder med op til 2500 fps for nogle applikationer og 1000 fps for voksne hjerte optagelser med fuld field of view imens en live præsentation af billederne vises på en skærm. T5 systemet blev brugt til at optage translations data som blev benyttet til validering af CFT-algoritmen. Disse billede sekvenser blev genereret ved hjælp af en høj-præcision translations scene med mulighed for horisontal og vertikal bevægelse i 10 μm intervaller, og en vævs-efterlignende fantom. Det den anden type billeder var fra HFR in vivo hjerteultralyds billeder med en billede-hastighed mellem 300 fps og 1000 fps.

Resultater: Studierne A og B præsenterede CFT algoritmen som gjorde det muligt at lave en præcis beskrivelse af bevægelse og deformation. Studie C var det første studie som viste statistisk signifikans i udbredelse af mekanisk kontaktion for patienter med normal echokardiografisk LV funktion: Den midterste del af septum. Disse identificerede kontraktion fronter bevægede sig konsistent hurtigere end elektrisk udbredelse gennem de elektriske veje og Purkinje netværk. Der blev udviklet en ny visualiserings metode, som blev kaldt Strain Rate Imaging (SRI). Strain raten fremhævede ændringer i myokardie deformationen, mens at præsentere dem som et billede således at de kunne visuelt inspiceres. Studie D fandt statistisk signifikans mellem kort-levede mekaniske events i patienter som var echokardiografisk normale, LBBB, og ikke-LBBB elektriske anormaliteter. Yderligere blev der udviklet en ny metode, som gjorde nytte af en modificeret korrelations koefficient, til at estimiere hjerte asynkronicitet. Korrelations koefficient viste statisk signifikante forskelle mellem patientgrupperne.

Konklusion: Det var muligt at identificerer mekaniske kontraktion fronter fra HFR B-mode echokardiografiske billeder. Forskellige kort-levede mekaniske events blev identificeret imellem forskellige patientgrupper. Til sidst blev det præcenteret hvordan strain kunne benyttes i sammenhæng med HFR echokardiografiske billeder til identificering a kort-levede og hurtigt udbredende mekaniske kontraktion fronter.

Contents

Preface

This PhD dissertation was written as an article-based thesis and represents the work conducted in the period of October 2015 and June 2019 at Aalborg University, Aalborg, Denmark. It was part of a collaboration between the Department of Health, Science and Technology at Aalborg University and the Department of Biomedical Engineering at Duke University. The PhD was internally supervised by the main supervisor Associate Professor Samuel E. Schmidt and the co-supervisor Professor Johannes J. Struijk. External supervisors were professor Olaf T. von Ramm at Duke University, Doctor Joseph Kisslo at Duke University Hospital, and Professor Peter Søgaard at Aalborg University Hospital. The PhD thesis was part of the "Cardiac Excitation Contraction Coupling" project, which was a multi-study project with collaboration between Aalborg University and Duke University. Data used in this study was acquired at Duke University Hospital. We extend our sincere thanks to the people and personnel, with special emphasis to Kristine Arges and Melissa LeFevre, at Duke University Hospital for the time, effort, and guidance during this project.

On the following pages you will find:

1. An introduction and background defining objectives.
2. A method section detailing the methodology and the data used.
3. A result section of the four studies.
4. Discussion and conclusion of studies.
5. Reference list of the four studies used.

Martin Vandborg Andersen
Aalborg University, August 19, 2019

List of Figures

List of Tables

List of Abbreviations

Abbreviation	Definition
1D	1 Dimensional
2D	2 Dimensional
3D	3 Dimensional
AHA	American Heart Association
ARF	Acoustic Radiation Force
AUC	Appropriate Use Criteria
BiV	Biventricular
CFT	Continuous Feature Tracking
CRT	Cardiac Resynchronization Therapy
CVD	Cardiovascular Disease
DALYs	Disability-Adjusted Life Years
ECG	Electrocardiography
EF	Ejection Fraction
ESC	European Society Of Cardiology
FOV	Field Of View
Fps	Frames Per Second
HF	Heart Failure
HF-pEF	Heart Failure With Preserved Ejection Fraction
HF-rEF	Heart Failure With Reduced Ejection Fraction
HFR	High Frame Rate
ICD	Implantable Cardioverter Defibrillator
IVS	Inter Ventricular Septum
LBB	Left Bundle Branch
LBBB	Left Bundle Branch Block
LV	Left Ventricle
LW	Lateral Wall
MI	Myocardial Infarct
Non-LBBB	Conduction disorder with no diagnosed Left Bundle Branch Block
NYHA	New York Heart Association
PSAX	Parasternal Short Axis
RBB	Right Bundle Branch
RBBB	Right Bundle Branch Block
RF	Radio Frequency
RV	Right Ventricle
SLBBB	Simulated LBBB
SWEI	Shear Wave Elasticity Imaging
SWI	Shear Wave Imaging
T5	Experimental High Frame Rate Ultrasound System Developed At Duke University
TDI	Tissue Doppler Imaging

Part I

Introduction

Chapter 1

Introduction

Cardiovascular Disease (CVD) is a large global burden on both human health and local and international economy. It is responsible for the loss of 64 million Disability-Adjusted Life Years (DALYs) every year in Europe alone [1, 2]. CVDs, including coronary artery disease, stroke, atrial fibrillation, heart valve disease, and Heart Failure (HF), are responsible for a large part of the global strain on society due to the requirements of long-term management and hospitalization [3, 4]. Diagnostic and treatment improvements are reducing mortality caused by cardiac diseases [5]. For example, the risk of death from coronary heart disease is projected to reduce by 30 % over the next 10 years. This is due to improvements in cardiovascular health metrics [1]. Acute CVD mortality rate has gone down due to the increase in short-term survival in acute hospitalizations. However, the prevalence of CVDs will increase in the coming years [3]. Morbidity and mortality rates associated with cardiac diseases are highly dependent on age, blood pressure, and cholesterol [6]. This means that the aging population in conjunction with the longer life expectancy of each individual in the western world will continue to increase the cost of long-term patient care [3]. For cardiac diagnostic purposes, in addition to the electrocardiography (ECG), deformation analysis from echocardiographic imaging provides diagnostic value when identifying patients with asynchronous cardiac contractions. The next generation of echocardiographic imaging revolves around describing waves and transient contractile patterns through the myocardium. Today, commercial deformation analysis using echocardiographic imaging is limited to frame rates below 100 images per second (fps), which is not adequate to resolve short transient events. To adequately resolve these events, high frame rate (HFR) imaging is required. Here, a temporal resolution of less than 2 ms is preferred [7]. The theory behind HFR is well-defined today. However, no commercially available solution exists to acquire and analyse this data. It is therefore not possible to take full advantage of the high temporal resolution to distinguish between normal and pathological patterns during transient contractile events.

Part II

Background

1 Cardiovascular Disease And Heart Failure

CVDs are the primary contributor to 3.9 million deaths, and account for 45 % of deaths in in the western world. With 11.3 million new CVD cases diagnosed annually in Europe alone, CVDs are responsible for 64 million DALYs annually, corresponding to 23 % of all DALYs lost. Past the age of 40, cardiac disease becomes the primary cause of morbidity and mortality in Europe and the USA. Cardiac diseases can lead to HF, a common condition with poor prognosis [8]. Today, 2.5 % of the adult population suffers from HF. Above 70 years of age, 10 % of the population in both Europe and the US have HF [9, 10].

HF is defined as a cardiac output deficiency so severe that the heart is unable to deliver adequate blood supply through the circulatory system. As a result, the heart cannot cover the body's organs' need for oxygen and nutrients [1]. Several factors, such as smoking, obesity, extremely low body weight, and blood pressure, have a significant negative impact on cardiac function and can be indicators of prevalent subclinical cardiac abnormal function [6]. Asymptomatic structural and functional cardiac abnormalities are two of the precursors to HF [10]. HF is characterized by classic symptoms such as shortness of breath, ankle edema from poor circulation, and elevated jugular venous pressure. These are related to structural or functional cardiac abnormality [10]. The New York Heart Association (NYHA) functional classification is a common tool of classifying severity of HF; see Table 1.1 [10].

Functional Classification Of Heart Failure

Class	Physical	Symptoms
Class I	No physical impairment.	No symptoms during normal physical activity.
Class II	Mild physical impairment.	Relatively comfortable at rest. Normal physical activity causes excessive breathlessness, fatigue, and palpitations.
Class III	Clear physical impairment.	Relatively comfortable at rest. Appearance of symptoms at light activity.
Class IV	Complete physical debilitation.	Can be symptomatic at rest. Any physical activity will increase discomfort.

Table 1.1: The table describes the New York Heart Association functional classification of heart failure [10].

When a patient is said to have HF, the patient has one of two types: HF with 'preserved' ejection fraction (EF) (HF-pEF), or HF with 'reduced' EF (HF-rEF) [10]. After patients are diagnosed with HF-pEF or HF-rEF, the mortality or remission rates are 35.3 % and 36.1 % in the first year after diagnosis, and

10 % in consecutive years [8–12].

2 Left Bundle Branch Block

Left untreated, HF will progressively worsen. If a patient develops asynchronous contraction between the Interventricular Septum (IVS) and Lateral Wall (LW), it causes severe deterioration of cardiac function. Left Bundle Branch Block (LBBB) is the obstruction of the Left Bundle Branch (LBB) and develops in 25 % to 30 % of HF patients. It brings with it a 70 % higher risk of sudden cardiac death [13]. LBBB is irreversible, so patients receive continuous treatment for the remainder of their lives if they are diagnosed with LBBB. It is, however, difficult to correctly identify true LBBB patients who will benefit from treatment, as several common conduction abnormalities can present as LBBB.

2.1 Electrical Excitation Of The Left Ventricle

When a normal heart contracts, an electrical action potential propagates through the Atrioventricular node and the Bundle of His. From the Bundle of His, the action potential splits into two electrical pathways: The Right Bundle Branch (RBB), and the LBB. The RBB transports an action potential towards the apex of the Right Ventricle (RV), while the LBB transports an action potential towards the apex of the Left Ventricle (LV). The LBB branches out into Purkinje fibers. Purkinje fibers themselves are located on the subendocardial walls of the ventricle. These cardiac fibers are specialized, like the bundle branches, in rapid propagation of electrical action potentials towards the cardiomyocytes with a velocity of 1 to 2 m/s [14]. This allows for the synchronous contraction of the ventricles [14]. When the electrical excitation reaches the cardiomyocytes, the electrical excitation propagation velocity is reduced to 0.3 to 0.6 m/s [14].

The cardiomyocytes deform producing the cardiac contraction. The duration of the QRS complex corresponds roughly to the duration required for complete electrical excitation of the LV. For patients with echocardiographic normal LV function, the QRS complex generally lasts 80 ms. The cardiomyocytes are electrically connected to each other by gap-junctions, allowing for sequential stimulation of the myocardium. This system is highly robust towards damaged tissue. When an obstruction of parts of the chain occur, as the action potential must arrive to the cardiomyocytes through other electrical pathways resulting in abnormal myocardial function [15, 16].

2.2 Obstructions In The Left Bundle Branch

An LBBB is an obstructed LBB, where excitation of cardiomyocytes is delayed. The LV action potential will not arrive through the LV Purkinje fibers. When the LBB is completely blocked, it is defined as a true LBBB. Here, the action

potential can no longer travel to the Purkinje fibers from the LBB. Instead, the action potential propagates through the RBB and travels through the IVS into the LV. This detour of the action potential results in prolonged duration for complete LV excitation and pathological electrical morphological patterns may occur [17]. The LBBB causes asynchronous contraction due to the delayed electrical excitation of the LV leading to a lowered stroke volume. For patients with LBBB the cardiomyopathy are still functional, meaning that the contraction occurs after the action potential propagates through the RV [14]. However, the asynchronous contraction results in increased mechanical work required of the LV in patients who often already suffer from HF. To maintain stroke volume, a progressive pathological remodeling of the heart occurs which leads to dilated cardiomyopathy. This is why LBBB has one of the most severe prognoses for patients with HF [13, 18]. Furthermore, the slow remodeling makes identification of LBBB in early stages of HF as patients often are asymptomatic [13, 18].

2.3 Diagnosis

In patients with LV systolic dysfunction, the pathological remodeling of the cardiomyocytes and extracellular matrix occurs slowly. Untreated systolic dysfunction is characterized as a progressive enlargement of the LV and a continuously decreasing EF. It is therefore often observed, that patients with mild symptoms may actually be in the high-risk group of hospitalization and death [10]. However, symptoms are non-discriminate, the diagnostic value is limited, and the functional classification of HF does not correlate well with the actual LV function. This is due to the non-specific nature of symptoms that cover a wide array of diseases [10]. Necrotic or scarred myocardial tissue does not contract if an action potential is introduced to the area. A pacemaker is, for this reason, not a viable treatment option for mechanical contraction abnormalities such as Myocardial Infarct (MI). Therefore, correctly distinguishing between electrical and mechanical dyssynchrony is crucial to improving treatment using Cardiac Resynchronization Therapy (CRT).

Detection & Diagnostics

LBBB patients often first show symptoms at late HF stages [10]. Here, pathological remodeling of the myocardium and extracellular matrix occur slowly after the onset of an injury to the electrical pathways. Because of this, untreated systolic dysfunction is characterized as a progressive enlargement of the LV and a continuously decreasing EF. Even when patients show symptoms, these are non-specific and do not help discriminate from other issues. Furthermore, specified symptoms are insensitive as they normally do not manifest in the early stages where primarily mild symptoms are present. Patients receiving diuretic treatments are asymptomatic and lack symptoms such as peripheral edema, making diagnosis harder [10]. This makes LBBB difficult to

diagnose, which is especially true in early stages of HF.

Two diagnostic tools are of interest when diagnosing patients with suspected LBBB and candidates for CRT: The ECG and kinematics using echocardiographic imaging [10].

Ventricular Classification Using Electrocardiography

The ECG describes the electrical function of the heart. The ECG provides detailed information about heart rhythms and electric conductivity, such as abnormal intra-ventricular conductivity. Today, treatment of LBBB is recommended for patients with a QRS greater than 150 ms. Patients with a narrow QRS below 130 ms are not recommended for LBBB treatment using CRT as they have shown a lower positive response rate to CRT [10, 16]. The refinement in LBBB detection has shown overall improvement in both morbidity and mortality. However, a large percentage of the patients receiving CRT do not show adequate response to make the treatment viable [16]. Selecting patients who will benefit from CRT is not a novel task. Therefore, a set of selection criteria has been derived by the American College of Cardiology Foundation to select patients for CRT and Implantable Cardioverter Defibrillators (ICDs). The goal was to group patients into two groups of patients: patients who benefit from CRT and ICD treatment, and patients who would be better off receiving no treatment [19]. The Apropriate Use Criteria (AUC) selection criteria are: QRS duration longer than 130 ms, LVEF lower than 35 %, and stage II-IV HF; see Table 1.2 [19].

Appropriate Use Criteria	
QRS duration	$\geq 130ms$
EF	$\leq 35\%$
NYHA	Stage II-IV HF

Table 1.2: Appropriate Use Criteria for cardiac resynchronization therapy (CRT). It is required that the patient meet the selection criteria requirements for QRS duration, ejection fraction (EF), and heart failure (HF) stage to be a candidate for CRT [19].

Patients are not selected for CRT if one or more of the AUC are not met; see Table 1.2. This means that HF-pEF patients will not be selected for CRT without extenuating circumstances as their chances of improvement are limited [9, 10, 19]. Between 30 % and 50 % of patients are misclassified as responders using the the AUC. This means that a patient who classifies as a responder either has no significantly positive response, or even has a deteriorated quality of life or life-expectancy, as a result of CRT [16, 17, 19–22].

Patients with other types of structural and physiological abnormalities generate electrical patterns resembling LBBB, while mechanical deformation patterns may signify patients with lower response rates to CRT [16, 23, 24]. Strict ECG criteria have been set for LBBB based on the electrophysiology of its al-

tered LV activation sequence: Prolonged QRS duration ($\geq 130ms$ and $\geq 140ms$ for women and men respectively) and Mid-QRS notching or slurring in at least two of the ECG leads [17]. There are differing opinions regarding strict ECG selection criteria. Bertaglia et al. 2017 concluded that the strict ECG selection criteria for CRT did not improve patient response to CRT. It should be noted that for Bertaglia et al. 2017 had a normal AUC specificity of 49 %, which is far lower than the normally reported CRT non-repsonse rates of 30 % [17, 22]. Jastrzebski et al. 2017 concluded a better prediction for survival compared to patients selected using the conventional AUC. They reported long-term mortality improvements in patients over an extended period of up to 7 year while having normal CRT response rate using conventional criteria [17, 25].

Ventricular Classification Using Echocardiographic Imaging

Echocardiographic imaging provides information about chamber volumes, ventricular and atrial systolic and diastolic function, wall thickness, and valve function [10]. The echocardiographic advantage compared to the ECG is the innate ability for visual assessment of the cardiac kinematics [26]. For diagnostic purposes, it is important to know which measurements can be expected for patients with echocardiographic normal LV function when trying to identify and understand an abnormal contraction [27]. Here 2 dimensional (2D) speckle tracking provides a tool for angular independent measurements of LV dimensions and myocardial deformation using strain [28]. New recommendations from the European Society of Cardiology (ESC) state that deformation imaging should be a standard measurement when assessing myocardial function [10].

Just like the strict ECG criteria, more detailed analysis of the mechanical deformation are of interest. Three mechanical deformation patterns show clinical promise due to potential clinical value; Early septal contraction, early stretching of the LW, and late LW contraction occurring after the aortic valve closure [15]. The combination of these patterns are often referred to as the septal flash. It generates a physical apical rocking of the LV due to asynchronous IVS versus LW contraction, which is often easy to visually asses using 2D B-mode [16]. Patients showing LBBB-like contractions may indicate that more specific and detailed contractile measurements should be used when diagnosing patients with asynchronous contraction.

2.4 Treatment

The first therapy step when a patient is diagnosed with LBBB is 3 months or more of guideline-directed pharmaceutical treatment. The hope is that the pharmaceutical treatment by itself improves LVEF so invasive steps will not be needed. Otherwise, CRT is considered the definitive treatment for patients when no significant benefit is observed from the medical therapy [5, 29].

Cardiac Resynchronization Therapy

CRT is an efficient technique for treating patients with asynchronous contraction caused by a electrical obstruction or delay. However, this therapy does not repair the electrical abnormalities, but instead provides an alternative and adjustable method for delivering the action potential to the cardiomyocytes using a pacemaker device. If the pacemaker device is deactivated, the asynchronous contractions reappear with an immediate onset. For biventricular (BiV) pacemakers, there is a RV and a LV lead. The RV lead is in the RV in an apical or septal position, whereas the LV lead is inserted through the coronary sinus into a, typically, lateral vein on the epicardial surface of the LV. This makes it possible to re-synchronize the cardiac tissue and thereby improve the cardiac output by reducing the amount of wasted work by the LV[19].

Short- and long-term survivability and quality of life are generally improved in HF patients who receive pacemaker implants today [20]. When the impaired mechanical contraction is identified and treated early, the reverse remodeling of the myocardium may, if not completely, revert to a healthier state [30, 31]. To avoid permanent pathological myocardial remodeling, it is imperative to identify asynchronous contraction so resynchronization of the myocardium can be performed as early as possible [30, 31].

3 State-Of-The-Art High Frame Rate Echocardiographic Imaging

HFR imaging has diagnostic value [32]. However, no clinically available systems are capable of HFR B-mode echocardiographic imaging above 200 fps for clinical applications. The cutting edge research today focuses on HFR deformation analysis. The primary goal is the electromechanical coupling of the LV due to its high potential prognostic value in cardiology.

3.1 Techniques And Limitations For High Frame Rate Echocardiographic Imaging

The conventional method for generating an image using a phased array is by emitting focused and directed transmit pulses and using beamforming to generate image lines. When the transmit pulse is focused, the reflected acoustic echo from the focused area will be stronger. The resulting echocardiographic images have higher spatial resolution and dynamic range. When the frame rate is increased, the transmit pulse must be widened so the resulting acoustic echo is reduced. There will always be a trade-off between temporal resolution and image quality, where the myocardial outline will be better defined at lower frame rates. For example, dropout of the myocardial walls may be more prevalent as temporal resolution increases. Figure 1.1 depicts a patient who had two image sequences acquired within 30 seconds from the apical four chamber view,

at 60 fps and 1000 fps respectively. Green circles in the two images illustrate how dropout of the Base of the IVS can occur.

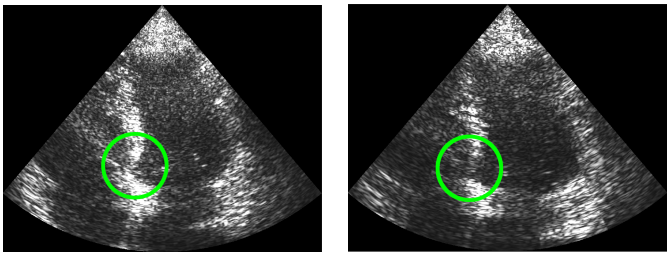

(a) 60 fps **(b)** 1000 fps

Fig. 1.1: Echocardiographic images from the apical four chamber view of a 45-year-old female with normal LV function. Figure 1.1a shows a frame without post-processing of the B-mode images when acquired at 60 fps. Figure 1.1b shows a frame without post-processing of the B-mode images when acquired at 1000 fps. The green circles illustrate how a higher temporal resolution may result in dropout from parts near the Base of the interventricular septum

HFR echocardiographic images consist mainly of speckles, which are caused by the scattering of acoustic energy within the tissue. It is often assumed that they are caused by sub-wavelength in-homogeneous objects causing reflection at fixed spatial locations. However, speckles have been shown to act more like artifacts, which are more dependent on the measuring system. It is often easier to imagine tissue as a homogeneous material with sub-resolution point scatters [33]. Speckles have randomly occurring patterns in the images, but the patterns are deterministic and can be reproduced exactly if the transducer array is returned to the same position using the same settings. The speckles are not accurate depictions of tissue. This is because of the speckles' dependency in the sub-wavelength tissue scattering and spatial location with respect to the transducer array [33]. This results in speckle patterns decorrelating as a function of distance and orientation with respect to the transducer array [34]. However, for small frame-to-frame translations, this reproducible feature of speckles makes them trackable and they may therefore be used for myocardial kinematics. This idea especially has merit for HFR as the frame-to-frame translation will be shorter compared to conventional echocardiographic imaging. Even though there is no a-priori information regarding the distribution of the speckle patterns, it is possible to track the myocardium between frames if the location of the myocardial contour in the initial frame is known.

Because the speed of sound remains constant in tissue, other methods for increasing imaging frame rate generation can be used. If it is a requirement that spatial sampling is not changed significantly, and image size must be preserved, there are three methods for increasing the temporal resolution of ultrasound [35].

Gated imaging is a method in which an ultrasound image is stitched together from M small image sectors acquired over M cardiac cycles. A focused

transmit pulse can be used for this approach, so the acoustic pressure available to generate image lines and the spatial resolution remains the same as for conventional ultrasound. However, this method has its limitations. Gating is highly sensitive to any motion by operator and subject, which can result in image artifacts between the image sectors. Gating also requires the patients to hold their breath M times as long compared to conventional ultrasound to reduce motion and stitching artifacts [35]. Gating is therefore unsuited for imaging of the heart, due to the high level of motion and unpredictable nature of many cardiac abnormalities such as arrhythmia and the physical limitations of HF patients [35].

Generating multiple transmit pulses is another approach used to increase frame rate. The limitations with this approach are the cross-talk between the multiple transmit pulses, resulting in ghost artifacts from other simultaneously acquired transmit pulses [35]. Spatial and spectral separation, frequency multiplexing, and apodization schemes have all been used to reduce cross-talk, but it remains a limitation of the method [36, 37].

Increasing 2D frame rates by parallel receive processing using computer tomography methods is called Exploso scanning, and it was first implemented for cardiac ultrasound in 1984 [38]. To generate enough acoustic pressure for all parallel receive-lines, transmit pulses are broadened to insonify a larger region per transmit pulse. This lowers the transmit resolution, but if receive resolution is maintained, the overall reduction of spatial resolution should be limited [35]. Today, Exploso scanning is one of the most commonly used methods for increasing temporal resolution in commercial systems [7, 35, 38–41].

Tissue Doppler Imaging

LV evaluation using Tissue Doppler Imaging (TDI) typically has a sampling rate of 150 Hz, while a sampling rate of 250 Hz can be achieved for single-wall analysis. The improvement of temporal resolution has been shown to increase the diagnostic value compared to conventional 2D B-mode images [32]. TDI measures movement and velocity in the transmit direction. This includes blood flow and tissue velocities, which may be used for diagnostic purposes [27]. Methods have also been developed to acquire high-speed TDI with 1 ms sampling [32, 36, 42]. The higher temporal resolution from TDI does come at a cost, as TDI inherently is 1 dimensional (1D). The method therefore suffers from the aperture problem, and any motion orthogonal to the transmit direction cannot be measured.

3.2 Wave Propagation

In vivo evaluations of propagating transient events have become clinically relevant as deformation analysis has improved in recent years [43–51]. Conventional ultrasound systems cannot resolve activation sequences adequately due to the low temporal resolution. HFR ultrasound provides the tool for detecting and

measuring the propagation and onset of these activation sequences. This makes it possible to correlate measurements with the ECG [7].

Derived information from ultrasound images, such velocity information from TDI and HFR ultrasound motion estimation algorithms, has been studied for several years. These studies aimed to describe transient waves in the myocardium in both animal and human studies [32, 39, 46, 50, 52–56].

Motion Estimation And Validation

Motion estimation validation can be tested by different methods. Today, real image data recorded using a translation stage from an ultrasound system is the golden standard for developing controlled translation data. Early approaches to developing synthetic images used non-rigid transformations to deform a single image, but the speckles in these images did not behave like speckles. In the last few years several synthetic ultrasound images developed using the Field II platform (Technical University of Denmark, 2800 Lyngby, Denmark) are capable of close approximations of real speckles. However, even the most advanced synthetic image formation methods remain approximations of speckles, and while they are publicly available, the image sequences are based on conventional low frame rate beamforming [57–60]. It should be noted that when contacted about generating HFR synthetic image sequences, these groups are willing to generate the point scatter datasets for you. So if you needed synthetic image sequences for your project you can generate the images yourself using Field II and their point scatter datasets.

To take full advantage of the HFR images, measurements emphasizing change should be used instead of global measurements such as EF and peak strain [61]. While velocity measurements emphasize changes, velocity measurements are unsuited to measure propagations of transient events in the myocardial walls, as they do not correct for overall cardiac motion [7]. Research groups have therefore in recent years been improving on methods for extracting measurements independent of overall cardiac motion such as strain and strain rate. These measurements emphasize local changes in the myocardium, as the overall cardiac motion may hide contractile information with clinical value [7, 32, 53].

Detecting Wave Propagation Using High Frame Rate

Several in vivo studies have been performed that demonstrate the feasibility and potential clinical utility of detecting short transient waves [62–65]. These include clinical feasibility and application of several techniques for measuring mechanical properties from echocardiography, such as myocardial stiffness [43–51]. Offline post-processing of the radio frequency (RF) data is commonly used for improving the image quality of the reconstructed ultrasound sequences and tracking accuracy of optical flow methods [66–69]. Shear Wave Elastographic Imaging (SWEI) is a non-invasive method for derivation of information regarding myocardial stiffness where the transient response of tissue from an induced

local change; stiffness and viscosity may be inferred [70]. SWI initially was used in conjunction with a mechanical push, like Acoustic Radiation Force (ARF). However, myocardial events such as valves opening or closing also produce shear waves that can be measured [54, 70].

Commercially, techniques for increasing frame rates are often accompanied by methods for increasing image quality [35, 40, 41]. The most prominent of these involve pre-processing using different image formation schemes like coherent compounding and harmonic imaging. They provide images with fewer speckles and more defined tissue structures [71, 72]. Coherent compounding is, as the name suggests, a compounding of multiple transmit pulses from different directions to reduce image clutter, but the method reduces temporal resolution. It is possible to have a high sampling rate using multiple compounded waves with a moving filter. Compounded frames will not be unique, unlike non-compounding methods, if a moving filter is used [66]. Resulting temporal resolution of the images for coherent compounding will still be equal to twice the duration for completing one unique frame [7, 66, 67]. Compounded images containing information from 5-frame windows of time and a cited frame rate of 500 fps effectively results in a temporal resolution equivalent to 100 fps. No additional temporal information benefits can be gathered beyond 100 fps. So, adding the non-unique frames between may just add computational load to the image analysis.

While harmonic imaging is non-linear, the tissue penetration of harmonic imaging is lower compared to fundamental frequency imaging, where signal amplitude may be 20 to 30 dB lower, which in turn requires the system to have a higher dynamic range and makes the system more susceptible to noise [73]. It is possible to combine both second harmonics and coherent compounding, which show improvements in tracking accuracy due to a 13 dB Signal to Noise Ratio (SNR) improvement [43]. Konofagou et Al. 2010 created a method, called electromechanical wave imaging, which uses RF data to automatically segment and estimate deformation of the myocardium [45, 50, 62, 74–76]. Electromechanical wave imaging has shown useful information at local regions in the myocardium. However, the RF data still requires motion along the transmit direction [62].

Duke University has an experimental phased array HFR ultrasound system, T5. It acquires images at up to 2500 fps while maintaining the live HFR 2D B-mode image presentation necessary during clinical scanning, which is unique to the von Ramm research group. The T5 increases frame rates using parallel hardware receive channels, where up to 32 image lines can be computed in parallel and in real-time, while having live images displayed [35]. However, the T5 did not have any deformation analysis software available. Therefore, a collaboration between Aalborg University and Duke University was planned where an algorithm was to be developed and validated for estimating kinematics of the LV using strain measurements derived from HFR B-mode images to describe transient mechanical wave propagations through the LV of the human heart. This was unique as in vivo human analysis of HFR B-mode echocardiographic images were not a focus of state-of-the-art HFR deformation analysis at the

onset of the project.

Chapter 2

Summary And Aim

1 Summary

Patients with HF are difficult to identify early as symptoms are non-deterministic and easily associated with less severe ailments. When patients are diagnosed with HF, correct treatment still remains difficult as many diseases have a similar diagnostic appearance by conventional measurements. Today, cutting edge diagnostic research focuses on fully determining electromechanical coupling. One of the objectives is to increase diagnostic value by identifying unique patterns to LBBB, as this is a common disease with very poor prognostic outcome for HF patients. Here, CRT therapy has a low specificity of 70 % or less. The H. Kanai group was the first to present propagating waves through the myocardial wall. Since then, multiple other groups have followed suit, as this area is highly under-determined. Today, research has not identified any transient mechanical waves, which have show diagnostic promise for characterizing differences between patients with echocardiographic normal LV function and LBBB patients. In order to describe short transient waves, HFR echocardiographic imaging is required. It enables the investigation of propagating waves in the myocardial wall [35]. Initially groups used motion and velocity information to describe these waves. They attempted to use strain measurements derived from HFR echocardiographic images as well, however, noise make HFR cardiac strain difficult to interpret due to the inherently low SNR of strain. Early attempts found limited success in tracking myocardial targets due to lower SNR. More recently, state-of-the-art HFR ultrasound-based strain measurements have produced more successful results. No manuscripts were identified comparing HFR transient events using echocardiographic images between different patient groups. Instead, the individual case studies of transient waves were used. These strain estimation algorithms required RF data. Using RF datasets results in huge datasets which are not clinically feasible for commercial systems. Extracting RF datasets also requires offline beamforming to recreate image sequences. The only system identified with online beamforming capa-

ble of live display visualization of the ultrasound images was the experimental phased array system, T5, developed at Duke University. This system did not give the user access to the RF data, but instead provided the enveloped data in ballistic coordinates. But no commercially available algorithms were identified that could analyze the T5 ultrasound image sequences. Therefore, a custom strain estimation algorithm was required if the T5 system should be used for research regarding in vivo transient wave propagation.

2 Aim

This thesis explored the possibility of extracting local transient information from HFR 2D B-mode echocardiographic images, and how deformation information could be visually assessed for identification of mechanical wave propagation. As a proof-of-concept, it offered methods for describing the cardiac function depending on cardiac health and the complexities affecting measurements.

3 Problem Formulation And Hypothesis

Problem Formulation 1: ***Is it possible to accurately track high frame rate cardiac deformation using B-mode echocardiographic images?***

Hypothesis 1: ***It is possible to estimate motion of high frame rate B–mode echocardiographic images while maintaining the tracking accuracy of current state-of-the-art algorithms which use radio frequency information.***

Problem Formulation 2: ***Can propagating mechanical waves be detected using B-mode echocardiographic images?***

Hypothesis 2: ***Mechanical waves propagating at 1 to 3 m/s can be identified using B-mode echocardiographic images.***

Problem Formulation 3: ***How can deformation information be visualized so propagation of mechanical waves becomes identifiable?***

Hypothesis 3: ***Deformation information can be presented in the manner of an image so that it emphasizes myocardial deformation changes.***

Part III

Methods

Methods

The paradigm of electromechanical coupling is under-determined in cardiology. The in vivo coordination of mechanical deformation varies greatly for conventional echocardiographic imaging. HFR 2D B-mode local transient kinematics is an area almost completely unexplored due to the physical and technical limitations concerning image formation. While there are research groups investigating HFR ultrasound, data is sparse and difficult to acquire. For this thesis, the only viable option was to use hypothesis-based quantitative research design with an exploratory approach to data acquisition.

4 Algorithm Design

Speckles are considered noise for most image modalities. However, ultrasound speckle patterns are deterministic. This means that the speckle patterns of a scene can be recreated exactly if a transducer is returned to a specific location and pointed towards the same direction. Due to the speckle patterns being sub-wavelength scatters in the tissue, the speckle patterns will decorrelate as a function of distance. However, for small frame-to-frame translations the speckle patterns will remain stable. Small frame-to-frame translation is a stronger assumption at HFR ultrasound imaging compared to conventional ultrasound imaging. This is due to the shorter temporal duration between image samples. Tracking individual speckle at HFR can therefore be a viable option for ultrasound kinematics.

In this project, we chose to focus solely on speckles as the method of detecting motion. The algorithm used a feature tracking approach. Here, all speckles identified within the ultrasound image sequences were used as features. Initially sparse sets of features were extracted from speckles. These features were tracked from frame to frame to create non-continuous speckle tracks for uniquely identified speckles. Myocardial motion was then estimated as a weighted average of the speckle tracks close to the points along the myocardial contour. This created an algorithm of low computational complexity, and made it well-suited for analyzing large datasets of thousands of images per cardiac cycle. The length of line approach to estimate strain curves from local regions along the myocardial contours was used to calculate myocardial

deformation at all points and time periods during the cardiac cycles.

5 Data Acquisition

5.1 The T5 Ultrasound System

Duke University's experimental phased-array ultrasound system (T5) was originally a real-time 3 dimensional (3D) system. It was repurposed to acquire HFR 2D B-mode.

The T5 system used a 3.5 MHz, 96-element, 18 mm wide, 1D phased array (Volumetrics, Durham, NC, USA) transducer. The theoretical diffraction-limited azimuth resolution was 1.2° and the axial resolution was 0.44 mm. Adequate Nyquist spatial sampling was maintained by angular sampling of 0.5° for a total Field Of View (FOV) of 80°. Axial sampling was 0.25 mm and scan depth was up to 140 mm depending on the patient. The T5 system used defocused transmit pulses focused at −30 cm (i.e. 30 cm behind the transducer) and 16 or 32 parallel receive processing channels per receive element, also known as 16:1 or 32:1 exploso scanning. This made the T5 system capable of acquiring images at up to 1000 fps while showing live images on screen; see Table 2.1. No compounding, apodization or harmonic imaging techniques were implemented. Data was exported from the system as detected B-mode 2D echocardiographic images in the native ballistic coordinate system.

Exploso Scan Summary	
16:1	10 transmit-receive operations were required to create an image. 500 images per second (I_{500})
32:1	5 transmit-receive operations were required to create an image. 1000 images per second (I_{1000})

Table 2.1: Summary of the difference in frame rate depending on the number of parallel receive processing channels per receive element.

A single lead ECG was recorded synchronously with the echocardiographic images. The ECG was used to manually identify the onset of the Q wave, which was defined as the zero time of each cardiac cycle. For an in-depth description on data acquisition using the T5 system, we refer to Moore et al. 2015 [35].

5.2 Patient Data Acquisition

The patient database of ultrasound image sequences was built and extended over a 5-year period between 2014 and 2018. Here, a set of 51 patients were

identified and recruited during routinely ordered echocardiographic examination at Duke University Hospital. This study was performed with approval from the Duke Institutional Review Board (Pro00026106) and approached using an independent recruiter. The patients were selected with the intent of acquiring HFR B-mode image sequences with high image quality relative to the standard T5 image quality to describe high temporal resolution mechanical contraction.

Definition Of Echocardiographic Normal	
QRS Duration	<100 ms
LVEF	> 50%
Atrial fibrilation	No
Cardiac function	Normal
Cardiac Anatomy	Normal
Valvular Stenosis	No

Table 2.2: Definition of patients with echocardiographic normal LV function.

Study A

Ten patients with different stages of cardiac health were recruited. HFR image sequences was consequently acquired from the apical four chamber view at 500 fps for 5 seconds with the T5 system by a trained sonographer.

For in vitro validation, two in vitro image sequences were created with the T5 system using a tissue mimicking phantom (CIRS Model 040GSE Multi-Purpose Phantom, Computerized Imaging Reference Systems, Norfolk, VA, USA). The phantom was imaged with a 3.5 MHz phased array transducer clamped to a high-resolution translation stage. Each generated image sequence contained 1000 frames with 10 μm between-frame increments for both horizontal and vertical translations. Nine regions of interest were selected manually in the images to avoid specular targets inside the tissue mimicking phantom. Different velocities could be simulated by excluding frames. For example, at 500 fps 10 μm increments correspond to 5mm/s. To simulate a 0.5 m/s velocity at 500 fps, every 100^{th} frame was used [77].

Study B

Two echocardiographic image sequences were acquired in the parasternal Short-Axis (PSAX) view at 365 fps from a 71 year old male LBBB patient with a BiV pacemaker. The BiV device was temporarily reprogrammed to intrinsic excitation and BiV pacing mode for each image sequence respectfully. This gave an initial comparison of intrinsic versus external pacing source in LBBB patients. It would also give preliminary results for exploring the possibility of using the PSAX view for diagnostic purposes [78].

Study C

Twenty patients with echocardiographic normal LV function were selected for Study C; see Table 2.2 for selection criteria. The patients were imaged in the apical four chamber view at 500 fps (I_{500}) and 1000 fps (I_{1000}) using the T5 system by a trained sonographer. The 500 fps images were only selected if the IVS and LW were not visible at 1000 fps. Three patients were excluded due to poor image quality. The final patient group consisted of 6 patients recorded at 500 fps and 11 patients recorded at 1000 fps [79].

Study D

Twenty-eight patients were selected for study D; see Table 2.3. The patients were divided into three groups: Thirteen patients with echocardiographic normal LV function, 9 LBBB patients, and 4 non-LBBB conduction disorder patients. All patients had images acquired during intrinsic conduction. Patients with LBBB and non-LBBB conduction disorder had a BiV pacemaker implanted and echocardiographic images of the apical four chamber view were acquired using two different pacing modes. LBBB patients had images acquired while being BiV paced, and non-LBBB conduction disorder patients had images acquired while RV paced apically to simulated LBBB. From every image sequence, 2 consecutive cardiac cycles were selected; see Table 2.4 [80].

Dataset Summary

	N	Included	Excluded
Patients	28	26	2
Datasets	81	75	6

Table 2.3: Patients and image sequences used in Study D [80].

Dataset Summary

Diagnosis	**Mode**	$\mathbf{N}_P$	$\mathbf{N}_D$
EchoNormal	-	13	26
LBBB	Int	9	17
	BiV		17
non-LBBB	Int	4	8
	sLBBB		7

Table 2.4: Summary of patients and image sequences from 26 patients. Here, the number of patients in each group is defined as N_P and image sequences in each group is defined as N_D [80].

Part IV

Study Contributions

Chapter 3

Study Contributions

1 Study A: Validation And First High Frame Rate In Vivo Results From Human Subjects

Study A described a novel method for analyzing the apical four chamber view using B-mode ultrasound images. The Continuous Feature-Tracking (CFT) algorithm focused on continuous tracking of features derived from speckles. The CFT algorithm was designed for analyzing the HFR B-mode images with simultaneously recorded ECG acquired by the T5 system. 2D or 3D images were required as several sections of the myocardium would be deforming horizontally, making low FOV or directional dependent methods unsuited. Furthermore, during the initial phase of the project, no conventional analysis algorithms or commercial software capable of analyzing the T5 data were available.

In vitro validation for both vertical and horizontal translations showed an underestimating motion near-field proximal to the transducer. Overestimation of motion in the far-field distal to the transducer was observed; see Figure 3.1. As translation increments increased above 0.7 mm/frame, tracking accuracy deteriorated; see Figure 3.2 [77]. The native ballistic coordinate system resulted in the size of speckles remaining constant through the image. However, sub-resolution translation estimation accuracy became increasingly important in the ultrasound far-field. The pixel-to-pixel motion of a field with uniform motion varied in a ballistic coordinate system with respect to range from the transducer. Take the pixel size of $[0.25mm, 0.5°]$ and a uniform vertical velocity of 0.5 mm/frame. At a range of 10 mm from the transducer, this would correspond to 5.7 pixels/fame. At a range of 120 mm from the transducer, this would correspond to 0.5 pixels/frame. Furthermore, speckles were more stable when moving in the axial direction. This was likely due to the variable axial pixel-to-pixel motion with respect to range [77].

In vivo beat-to-beat reproducibility was calculated for 6 myocardial segments along the myocardial contour by analyzing complete cardiac cycles dur-

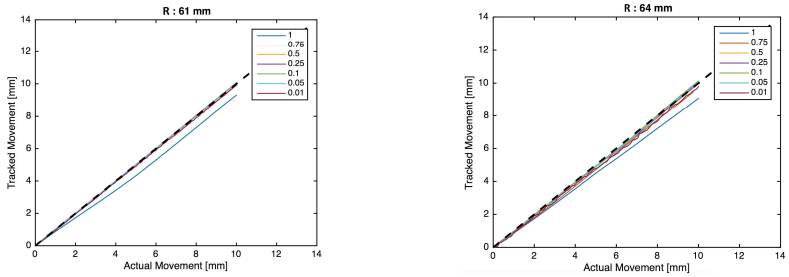

(a) Vertical Tracking Results **(b)** Horizontal Tracking Results

Fig. 3.1: Vertical and horizontal translation estimations versus true translations. The data was derived using a tissue mimicking phantom and a high precision translation stage. R is the ROI's distance from the transducer array, and line labels represent frame-to-frame translation increments [77].

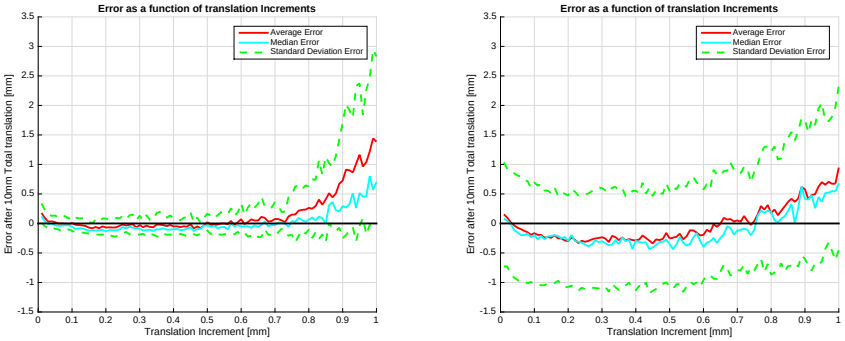

(a) Vertical Tracking Results **(b)** Horizontal Tracking Results

Fig. 3.2: Vertical and horizontal translation estimations versus true translations. The data was derived using a tissue mimicking phantom and a high precision translation stage [77].

ing the 5 second image sequences. The cardiac cycles were segmented and analyzed individually, and the averaged Fishers' z transformed correlation coefficient was used to describe reproducibility for each segment. Reproducibility results showed an averaged correlation coefficient of 0.95 across all myocardial segments and patients [77]. Two early stretch phases were identified in the image sequences; see Figure 3.3. It is unknown why these stretches occur. However, micro-contractions were often observed during slow motion playback of the B-mode images, of which a small video clip was attached to the manuscript. We were therefore confident that these stretches related to real mechanical events during isometric contraction and not artifacts from the tracking algorithm [77]. One potential origin could be atrial relaxation causing a slight deformation in the mitral valves causing a small change in LV volume.

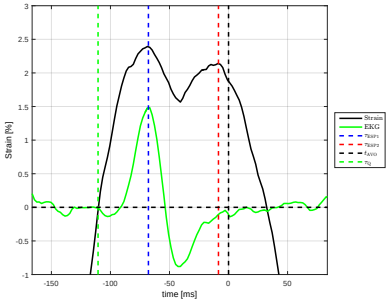

Fig. 3.3: Mid-septal wall strain curve for a 200 ms period during and after the QRS complex for a 49-year-old male with normal LV function showing two clearly defined early stretch phases illustrated by the blue and red horizontal lines [77].

2 Study B: Circumferential Strain

There were inconsistencies in the literature for which cardiac views provide the highest predictive value with respect to myocardial function and heart failure [81, 82]. The largest limitation with the PSAX view is the high intra- and inter-operator variability, which in part is due to the lack of identifiable landmarks. This makes reproducible PSAX strain measurements difficult. PSAX does offer a different but interrelated descriptor of the mechanical contraction [81, 82]. Study B described the implementation of circumferential strain estimation in the PSAX view using the CFT algorithm to show that the CFT algorithm was angular independent.

It was arduous to acquire high quality images from the PSAX view. This was likely due to the orientation of myocardial fibers resulting in fewer borders where the sound could be reflected. Circumferential strain could be estimated from HFR echocardiography using the CFT algorithm [78]. By introducing a Kalman Filter for myocardial wall tracking, a-priori information from previous frames were used when valid speckle tracks were sparse, providing a more robust implementation of the CFT algorithm compared to the 2015-2016 version [77, 78]. A LBBB patient with a BiV pacemaker was selected for data analysis. The patient was acquired in the PSAX view, both during intrinsic excitation and BiV pacing. Here, the duration of tissue shortening remained constant between intrinsic conduction and BiV pacing, supporting the fact that the patient's asynchronous contraction was caused by an electrical block and not a mechanical defect such as an MI. The study also showed proof that the algorithm was not angular dependent for analyzing myocardial kinematics [78]. The general image quality from the PSAX view did present a significant problem. It was therefore concluded that the PSAX view should not be used for further algorithm analysis before image quality could be improved [78].

3 Study C: High Frame Rate Analysis Of Patterns For Patients With Normal Left Ventricular Function

Study C described differences in the onset and duration of mechanical events for patients with echocardiographic normal LV function using HFR echocardiographic images. The study presented a comparison analysis of strain curves from 17 patients with echocardiographic normal LV function, ages 42 ± 17 [79]. A naive approach was used to define the onset of myocardial events. The naive approach to identifying myocardial events reduced the subjectivity of the measurements [79].

The analysis for tissue shortening onset the measurements showed the myocardial segments were significantly different ($P < 0.01$) between groups. Multiple comparisons showed the mid septal segment contracted significantly earlier compared to the other 5 myocardial segments. Tissue isometric relaxation interval also showed significantly different ($P = 0.03$) measurements between groups. Multiple comparisons showed the basal septal segment duration was significantly longer compared to the other 5 myocardial segments [79]. These results resemble results by other groups [32, 42, 53]. A propagating velocity of 5.6 m/s was measured [79]. This was high compared to the propagation of the electrical wave front through the Purkinje network of 1 to 3 m/s. Several interactions with the myocardial contraction could have effected the observed propagation velocities. These include multiple locations of excitation breakthrough between the Purkinje network and myocytes, the afterload of the LV, and the visual limitation with a 2D imaging plane [14, 47, 56]. It is assumed that the three interactions mentioned may have a role to play in the consistently high propagation velocities. Six different isometric patterns were identified during the study; see Figure 3.4. It was assumed that the patterns may be an effect of RBB and LBB interaction together with pre- and afterload of the LV [79].

4 Study D: High Frame Rate Transient Contraction Fronts In Patients

The feasibility of detecting contractile activation patterns was investigated in this study. This was done using a group of 13 patients with echocardiographic normal LV function, 9 LBBB patients, and 4 non-LBBB conduction disorder patients [80].

A method was presented for identifying visual changes in transient contractile patterns through the IVS depending on pacing modes. The Strain Rate Images (SRI) were derived from strain rate curves along the myocardial contours. A pixel within the SRIs corresponded directly to the strain rate at a specific time and location within the myocardial wall [80]. Propagating

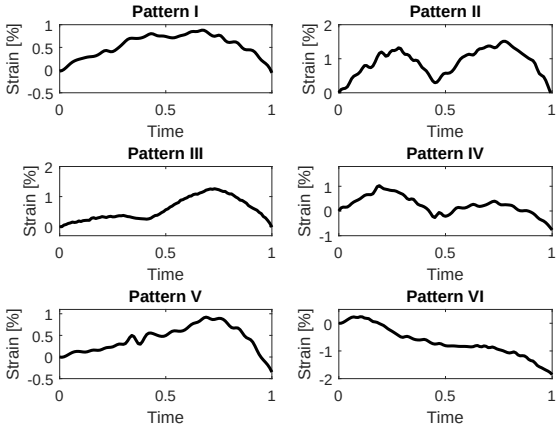

Fig. 3.4: Isometric contractile patterns identified after the first Q wave deflection. Time windows were normalized with respect to the isometric contraction [79].

fronts were emphasized using a colormap with hot and cold colors. When a color changed from cold to warm color, or vice versa, it indicated myocardial deformation change and the onset of a new transient event. Fine spatial sampling of strain curves made it possible to resolve and distinguish between the propagation transient contractile fronts [80].

Patients with echocardiographic normal LV function appeared to have more homogeneous SRIs compared to patients with LBBB and non-LBBB conduction disorder; see Figures 3.5 & 3.6. However, no consistent transient patterns were identified for patients with echocardiographic normal LV function [80].

Two propagating stretches were observed during the isometric contraction. These patterns were reported previously; see Figure 3.3 [77]. Myocardial tissue shortening happened during the first contractile front, but the first stretch often appeared prior to the Q wave. This was especially true for patients with LBBB and non-LBBB conduction disorder. This makes the initial stretch unlikely to be onset of mechanical contraction [80]. The front may potentially be the relaxation of the atria, or asynchronous RV-LV contraction. Some patterns only manifested in patients with non-LBBB conduction disorder and LBBB. For example, a prolonged temporary cessation of the tissue shortening, often accompanied by an early myocardial stretch prior to the QRS complex, was often observed in the patients with non-LBBB conduction disorder and LBBB [80]. Different transient patterns of the second contractile front were identified between patients. While some transient contractile fronts were repetitive for consecutive cardiac cycles intra-patient, no definitive consistent morphologies were observed inter-patient [80].

An electrical excitation through the Purkinje network generated fast propagating contractile fronts. When an action potential was redirected through the cardiomyocytes, the propagation velocity was significantly slower. This was

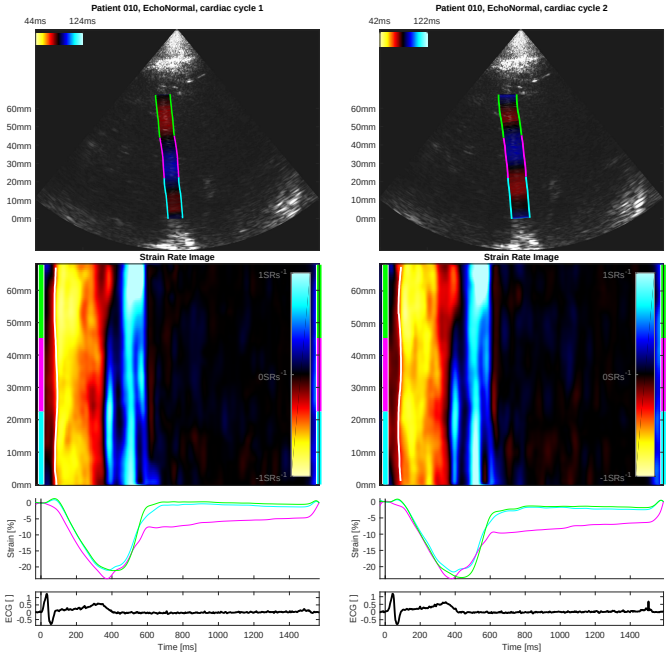

(a) Cardiac Cycle #1 **(b)** Cardiac Cycle #2

Fig. 3.5: Strain rate images (SRI) derived from a 21-year-old male. The patient was considered normal from an echocardiographic perspective. Figures 3.5a & 3.5b show two consecutive cardiac cycles from a 5 second recording. The 2D correlation coefficient between the two SRIs was calculated to $c_\star = 0.96$ [80].

reflected in the duration of the tissue shortening propagation through the IVS between patients with echocardiographic normal LV function (25.2 ± 10.0 ms, P<0.01) and patients with non-LBBB conduction disorder [80].

A measurement to indicate asynchronous contraction using the correlation coefficient ($c_\star$) of the SRI was implemented. $c_\star$ described the correlation coefficient between the SRI and a spatially mirrored version of itself; see Equation 3.1 [80]. Patients with echocardiographic normal LV function had significantly higher $c_\star$ ($c_\star = 0.67 \pm 0.04$, P<0.01) compared to patients with conduction disorders, which indicated high synchrony in the contraction through the IVS [80].

$$c_\star(A) = \frac{1}{S+T-1} \sum_{s=1}^{S} \sum_{t=1}^{T} \frac{(\overline{A_{(t,s)}} - \mu_A)(\overline{A_{(t,S-s)}} - \mu_A)}{\sigma_A^2} \tag{3.1}$$

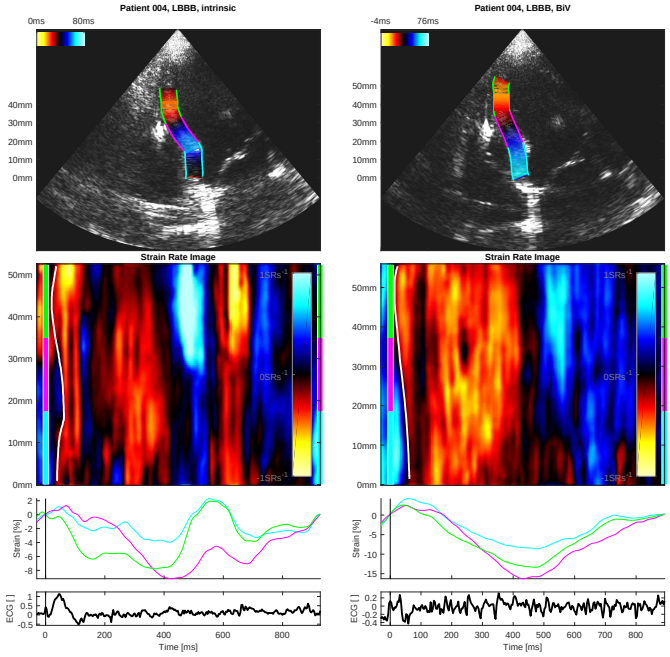

(a) Intrinsic Conduction **(b)** Biventricular Excitation

Fig. 3.6: Strain rate images (SRI) derived from an 85-year-old female with left bundle branch block and a biventricular (BiV) pacemaker. Figures 3.6a & 3.6b show the SRIs of the patient during intrinsic conduction and BiV pacing respectively. The 2D correlation coefficient between the two SRIs was calculated to $c_\star = 0.40$ with intrinsic conduction and $c_\star = 0.68$ for BiV excitation [80].

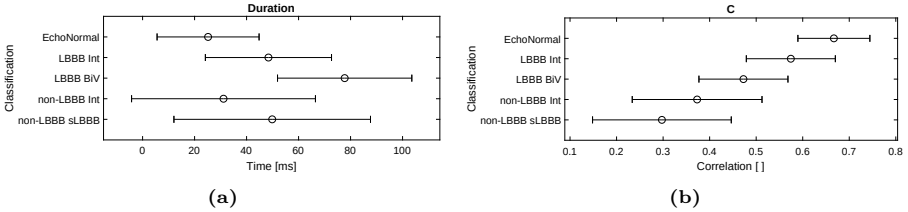

(a) **(b)**

Fig. 3.7: Averages for duration and correlation coefficients divided into 5 groups. Subfigure 3.7b illustrates the duration of tissue shortening onset propagation through the IVS, and Subfigure 3.7a describe the correlation coefficients the SRI as defined by Equation 3.1 [80].

Several measurements associated with both synchronous contraction and the duration of contractile front propagation were identified. The transient contractile front of patients with echocardiographic normal LV function (25.2 ± 10.0 ms) were shorter than the 45 ms expected for electrical excitation propagation through the Purkinje fibers. However, significantly shorter transient contractile fronts for patients with echocardiographic normal LV function com-

Multiple Comparison For Duration

Diagnosis	Mode	μ [ms]	σ [ms]	p	p_{Log10}
EchoNormal	-	25.19	10.01	-	-
LBBB	Int	48.41	12.38	0.59	0.01
	BiV	77.73	13.18	0.02	<0.01
non-LBBB	Int	31.13	18.04	1.00	0.99
	sLBBB	49.86	19.29	0.79	0.03

Table 3.1: Results of the multiple comparison duration measurements. Averages and standard deviations of all measurements are reported. Post-hoc Bonferroni corrected multiple comparisons were calculated for patients with echocardiographic normal LV function versus patients with conduction disorders. p values < 0.05 were considered significant [80].

Multiple Comparison For Correlation Coefficients

Diagnosis	Mode	μ [ ]	σ [ ]	p	p_{Log10}
EchoNormal	-	0.67	0.04	-	-
LBBB	Int	0.57	0.05	0.58	-
	BiV	0.47	0.05	0.02	-
non-LBBB	Int	0.37	0.07	<0.01	-
	sLBBB	0.3	0.08	<0.01	-

Table 3.2: Results of the multiple comparison correlation coefficient measurements. Averages and standard deviations of all measurements are reported. Post-hoc Bonferroni corrected multiple comparisons were calculated for patients with echocardiographic normal LV function versus patients with conduction disorders. p values < 0.05 were considered significant [80].

pared to simulated LBBB (49.9 ± 19.3, P=0.03), LBBB patients with intrinsic excitation (48.4 ± 12.4, P=0.01), and LBBB patients with BiV excitation (77.7 ± 13.2, P<0.01), were measured. This indicated slower propagation through the IVS when electrical excitation originated from the RV [80].

For some LBBB patients, individual segments of the myocardium showed improved contractions from the BiV excitation while the IVS had an impaired contractile function due to a worsened asynchronous contraction through the IVS [80]. Comparing patients with echocardiographic normal LV function (0.67 ± 0.04) to non-LBBB conduction disorder with intrinsic excitation (0.37 ± 0.07, P<0.01), simulated LBBB (0.3 ± 0.08, P<0.01), and LBBB patients with BiV excitation (0.47 ± 0.05, P=0.02), the modified correlation coefficients were significantly higher (P<0.01); see Figure 3.7. This implied more synchronous contractile patterns [80].

Part V

Discussion And Conclusion

Chapter 4

Discussion

Echocardiographic imaging is a mature technology that has been used for non-invasive real-time cardiac diagnostics since the early 1970s. Commercial phased array ultrasound system focuses on improving image quality of ultrasound. The high temporal resolution of echocardiography makes it well suited for estimation of myocardial kinematics. Echocardiographic images make it possible to resolve myocardial states through the entire cardiac cycle. Fully imaging the LV often requires a wide FOV of 90° or more. Here, myocardial motion at the apex can be orthogonal to the transmit pulse, making 1D modalities such as TDI unsuited analysis modalities.

The aim of this thesis was to detect propagation of transient mechanical waves associated with electromechanical coupling using HFR 2D echocardiographic images.

Manuscripts Story Line

Increasing temporal resolution of echocardiographic imaging has severe image quality drawbacks. For ultrasound images, the image quality is proportional to the acoustic pressure of the transmit pulse. As the transmit pulse is widened, the regulation limitations with respect to the mechanical index. The mechanical index limits the acoustic pressure which can be emitted into the body due to the risk of myocardial bioeffects. This results in a lower local acoustic pressure for generation of the image lines. High computational requirements of HFR ultrasound also results in an offline beamforming approach being used. Offline beamforming makes accurate acquisition of specific cardiac views difficult compared to conventional ultrasound. The difficulty arises from the system operator being blind during acquiring HFR images, and the quality of the image sequences being unknown before beamforming. The advantage of using this approach is the reduced computational requirement of the ultrasound system. Where the T5 system shined, compared to its counterparts, was the capability of showing live images while acquiring HFR echocardiographic sequences,

which are essential for clinical evaluation. This was achieved using online and real-time beamforming. The primary limitation to this approach was that the T5 did not provide a method of extracting RF data, but only B-mode image sequences.

Due to continuously recruitment requirement of patients, the T5 system was selected to be the best fit for the lifespan of the project.

Study A and B: Validation Of Deformation Estimation Algorithm
A deformation algorithm, with similar tracking performance to the available software, was designed for data analysis due to limitations of the T5 system. The algorithm was designed to extract myocardial kinematics of the LV for one cardiac cycle using HFR B-mode echocardiographic image sequences. The primary focus of the algorithm was to accurately track sub-pixel motion of the myocardium to calculate transient deformation propagation for adult HFR deformation imaging acquired in vivo. Tracking accuracy of the CFT algorithm was measured using translation images. These images were generated using a tissue mimicking phantom positioned on a translation stage. High accuracy and precision were measured when comparing the translation estimations to the physical translation. Tracking motion across image lines were less accurate compared to tracking axial motion.

The capability of analyzing images independent of transducer orientation was shown by a small second study. In vivo reproducibility measurements for HFR cardiac strain curves were measured as well. These results were comparable with today's state-of-the-art RF sequence tracking algorithms [45]. The algorithm was capable of estimating motion along the entire PSAX. However, the image quality from the PSAX views were generally poor. This was likely caused by the myocardial fiber orientation reducing the reflective structures in the myocardium. PSAX views were therefore ill-suited for our proof-of-concept development. It was shown that the no assumptions needed to be made to estimate deformation using the CFT algorithm. Algorithms using RF data inherently describe axial information, and therefore may require assumptions to measuring off-axis kinematics [83–85].

Study C: Describing Transient Events In Ehocardiographic Normal Left Ventricles
Patients with echocardiographic normal LV function had been used in multiple HFR studies before Study C. In prior studies, patients were analyzed as individual case studies so no statistical differences were identified between patients. The next step was therefore to identify parameters which could be compared between patient groups. Four unique sets of measurements were identified occurring in all patients with echocardiographic normal LV function.

Six different deformation patterns were identified in this study during isometric tissue shortening. These patterns could potentially lead to subjective decision-making with regard to onset and duration of myocardial events such as tissue shortening onset. These events were defined using a strictly objec-

tive approach for identifying the onset of mechanical events. This provided a tool for creating reproducible measurements of onsets and duration of mechanical events. The method had limitations such as over- and underestimation of temporal events. However, the estimation errors were accepted to reduce subjectivity.

This was to our knowledge the first time patients with echocardiographic normal LV function were studied using HFR echocardiographic images where a intra-patient comparison showed statistically significant differences between myocardial segments. The significant differences in duration and interval measurements described in Study C cannot be identified using commercially available strain analysis. The temporal resolution of commercial systems is normally 17 ms, corresponding to 60 fps, and would have been insufficient for resolving the duration of the short transient differences between myocardial segments of 13.2 ms for the tissue shortening onset measurements. Higher temporal resolution of 500 fps or above was therefore essential for adequately resolving and describing the events.

Study D: Differences Between Normal Left Ventricular Function, LBBB, And Non-LBBB Conduction Disorder Patients

Conventional strain curves limit the information that can be visually extracted. This is due to two primary issues with presenting the data. First, the curves inherently overlap. If they are plotted individually, it is exceedingly difficult to compare multiple curves. Secondly, it was difficult to identify unique transient contractile fronts using conventional strain curves. A structured method of visualizing the deformation information was needed. During the initial data analysis of Study C and Study D it became apparent that high spatial sampling would be beneficial. This would help identify propagating mechanical contractile fronts. The data needed to have a well-ordered visualization method such as an image. This would make visual identification of the propagating contractile patterns possible. Therefore, a method was developed for visualizing the strain rate using a SRI to further emphasize changes.

Using SRIs, it was possible to detect significant differences in measurements for asynchronous contraction along the IVS when comparing patients with echocardiographic normal LV function against LBBB and non-LBBB conduction disorder patients. This was done using a modified correlation coefficient defined in Equation 3.1. The modified correlation coefficient has the potential for early indication of asynchronous contraction.

Unique Scientific Contribution

This thesis and accompanying manuscripts provided a new take on HFR speckle tracking. While most HFR algorithms require the use of RF sequences, the CFT algorithm only required the use of B-mode image sequences, making it less computationally heavy. The algorithm uses a naive approach to speckle tracking. It uses the peaks of the speckles as the center, and the average motion

of multiple speckle tracks to estimate myocardial motion. This simple approach showed tracking results comparable with current state-of-the-art algorithms used for HFR echocardiographic kinematics. Multiple studies mentioned using motion estimation for describing transient mechanical events. However, prior to Studies A through D, velocity and translation were the primary measurements used for cardiac analysis. These measurements are poorly suited for extracting information regarding regional myocardial measurements. Our studies strictly used in vivo HFR deformation imaging using strain from the human LV. The studies were the first to compare and show statistically significant differences between patients with echocardiographic normal LV function, LBBB, and non-LBBB conduction disorder patients by using HFR SRIs.

During isometric contraction, two short transient stretches of the myocardium occurred. While this thesis mentioned these stretches on multiple occasions, they are still underdetermined. Several studies presented data with an indication of these stretches [86]. However, no mention of the patterns were observed. This was likely due to the stretches normally being associated with noise. These stretches potentially have three causes: The first possibility was an RV-LV dyssynchrony causing a contractile propagation through the RV. The second possibility was the closure of the mitral valve causing a small change in pressure, resulting in a small early stretch of the LV. The third possibility was cessation and relaxation of the left atria causing a small morphological change to the mitral valve. These early stretches require further investigation to determine their origin to improve electromechanical coupling research.

Perspective For High Frame Rate Echocardiographic Imaging

The initial hypothesis regarding contractile front propagation was naively chosen with respect to the cardiac electromechanical physiology identified from electrophysiology. Here the electrical excitation propagates at between 1 and 3 m/s through the LBB and Purkinje network, and 0.3 to 0.6 m/s through the cardiomyocytes. It is generally understood that the first electrical excitation of cardiomyocytes would occur roughly half way between the Base and the Apex of the IVS. Therefore, our assumption and expectation were that: A clearly defined transient contractile front propagating through the LV would be observed. Propagation velocities would correspond to the electrical properties of the medium that the action potential propagated through. For example, for patients with echocardiographic normal LV function the propagation velocities would correspond to electrical excitation through the Purkinje network. For LBBB patients, the hypothesis was that the electrical excitation would propagate from the RV and via the cardiomyocytes into the LV. It was expected that this generated a propagating velocity corresponding to cardiomyocyte excitation propagation of around 0.6 m/s, or roughly half the propagating velocity compared to normal healthy conduction. These assumptions did not hold as our results indicate.

An interesting observation was the differences in transient mechanical events

between patients with echocardiographic normal LV function and LBBB patients. No HFR measurements for identifying propagating differences between patients with echocardiographic normal LV function and patients with LBBB or simulated LBBB were found. It was shown that transient mechanical contractile fronts through the LV in most patients were shorter than what could be attributed to electrical excitation propagation through the Purkinje network. Significantly higher propagating velocities were measured, and multiple contractile onset locations were observed in some patients.

It has become inherently clear that the HFR deformation imaging field is under-determined. Further improvements in cardiac diagnostics require mapping of transient mechanisms. In future studies, using an animal model to determine the isometric contraction phase to explore how the two stretch phases occur is suggested. This could allow accurate prediction of propagation origin and velocity on a patient-to-patient basis. These questions could not be answered in this dissertation. However, a tool using kinematics of HFR echocardiographic imaging potentially capable of answering them with further investigation was developed to further explore myocardial deformation.

1 Limitations

It was not possible to uniquely identify how different mechanical abnormalities affect the mechanical contractile front propagation through the ventricle due to the limited number of patients and image sequences available. This will be of utmost importance to have a larger population of patients with deep insight into their cardiac health when identifying HFR measurements with diagnostic and prognostic value.

To accurately describe electro-mechanical coupling, a synchronous 12-Lead ECG recording would have been well-suited. However, only a single-lead ECG was available for this thesis. The onset of tissue shortening propagation was highly dependent on the appearance of individual ECG recordings and how the onset of the cardiac cycle was defined. An abnormal ECG made the onset of electrical activation difficult to identify in most cases. Defining the correct onset for the cardiac cycle may therefore be of absolute importance. We suspect that a 12-lead ECG would help improve this, and suggest that this may be an important improvement when evaluating HFR echocardiographic images, while also having the potential of being used for mapping electromechanical coupling evaluation.

The inherently reduced image quality of HFR echocardiographic images often made patient selection difficult, as image dropout often occurred in multiple walls. Deformation analysis is normally done using image sequences from multiple cardiac views such as apical two and three chamber views. Using the two other apical views would provide a 16- or 18-segment model, and can provide increased insight into myocardial contraction. However, the limited image quality resulted in the apical four chambers being the view with the highest

image quality and least amount of dropout within the echocardiographic image sequences. For our studies, only the apical four chamber view was therefore used. The measurements in these studies described when the LV pumps blood into the Aorta, and hence may not be directly associated with electrical excitation.

Extracting image planes of the myocardial wall will generally confound contractile front propagation determination. This is due to the 3D myocardial structure being under-determined in lower dimensions. The 3D myocardial structure is confounded if the contractile front propagation determination technique is limited to fewer dimensions, which includes both 1D and 2D echocardiography. However, no systems were capable of HFR 3D echocardiographic acquisition. Describing transient mechanical events in 3D were therefore not an option, so 2D description of the transient contractile fronts were the best alternative.

Using enveloped data for deformation analysis further confounded tracking as it restricted the algorithms from using phase and envelope for kinematics.

Chapter 5

Conclusion

This thesis may set the groundwork for further electromechanical coupling research. Studies were presented exploring the possibility of detecting and describing in vivo mechanical contractile front propagation within the LV of the heart associated with electrical excitation. An algorithm was described and tested for extracting deformation information from HFR 2D B-mode echocardiographic image sequences from different myocardial views. These studies showed reproducible results similar to current state-of-the-art methods for measuring deformation using HFR 2D B-mode echocardiographic imaging. This was the first time statistically significant differences between myocardial segments of the LV during the cardiac cycle in patients with echocardiographic normal LV function was measured. It was possible to detect mechanical contractile fronts using HFR 2D B-mode echocardiographic images that could not be adequately resolved using conventional temporal resolution. Consistently shorter transient events were observed for propagating contractile fronts compared to known cardiac physiology, hinting at other forces affecting the contractile front and the need for HFR 3D echocardiographic imaging.

As the number of strain curves increased, conventional deformation analysis became overwhelmingly complex for the human eye to interpret due to the amount of record keeping required to understand the strain curves. Interpreting high spatially sampled deformation information was instead done by visualizing mechanical contractile front propagation as a SRI. A new and automated measurement of contractile synchrony using a modified correlation coefficient was defined and showed significant differences between patients with echocardiographic normal LV function and patients with LBBB and non-LBBB conduction disorders.

The hypothesis of mechanical fronts propagation being directly comparable to electrical excitation did not hold. However, it was possible to show statistical differences that may be of diagnostic value, which could not be identified using conventional echocardiographic images, and that mechanical contractile front propagation should be measured using HFR echocardiographic imaging and

deformation analysis.

References

[1] F. Emelia J. Benjamin, MD, SCM, M. Michael J. Blaha, MD, S. Stephanie E. Chiuve, F. Mary Cushman, MD, MSc, F. Sandeep R. Das, MD, MPH, M. Rajat Deo, MD, M. Sarah D. de Ferranti, MD, M. James Floyd, MD, F. Myriam Fornage, PhD, and M. Cathleen, "Heart Disease and Stroke Statistics—2017 Update," *Circulation*, vol. 135, no. 10, pp. 1—-775, 2017.

[2] E. Wilkins, L. Wilson, K. Wickramasinghe, P. Bhatnagar, J. Leal, R. Luengo-Fernandez, M. R. R Burns, and N. Townsend, *European Cardiovascular Disease Statistics 2017 edition.* European Heart Network, 2017.

[3] S. Bansilal, J. M. Castellano, and V. Fuster, "Global burden of CVD: Focus on secondary prevention of cardiovascular disease," *International Journal of Cardiology*, vol. 201, pp. S1–S7, 2015.

[4] J. Loader, Y. K. Chan, J. A. Hawley, T. Moholdt, C. F. McDonald, P. Jhund, M. C. Petrie, J. J. McMurray, P. A. Scuffham, J. Ramchand, L. M. Burrell, and S. Stewart, "Prevalence and profile of "seasonal frequent flyers" with chronic heart disease: Analysis of 1598 patients and 4588 patient-years follow-up," *International Journal of Cardiology*, vol. 279, pp. 126–132, 2019.

[5] E. Sze, Z. Samad, A. Dunning, K. B. Campbell, Z. Loring, B. D. Atwater, K. Chiswell, J. A. Kisslo, E. J. Velazquez, and J. P. Daubert, "Impaired Recovery of Left Ventricular Function in Patients With Cardiomyopathy and Left Bundle Branch Block," *Journal of the American College of Cardiology*, vol. 71, no. 3, pp. 306–317, 2018.

[6] H. Dalen, A. Thorstensen, P. R. Romundstad, S. A. Aase, A. Stoylen, and L. J. Vatten, "Cardiovascular risk factors and systolic and diastolic cardiac function: A tissue Doppler and speckle tracking echocardiographic study," *Journal of the American Society of Echocardiography*, vol. 24, no. 3, pp. 322–332.e6, 2011.

[7] M. Cikes, L. Tong, G. R. Sutherland, and J. D'Hooge, "Ultrafast cardiac ultrasound imaging: Technical principles, applications, and clinical benefits," *JACC: Cardiovascular Imaging*, vol. 7, no. 8, pp. 812–823, 2014.

[8] P. A. Heidenreich, N. M. Albert, L. A. Allen, D. A. Bluemke, J. Butler, G. C. Fonarow, J. S. Ikonomidis, O. Khavjou, M. A. Konstam, T. M. Maddox, G. Nichol, M. Pham, I. L. Piña, and J. G. Trogdon, "Forecasting the Impact of Heart Failure in the United States," *Circulation: Heart Failure*, vol. 6, no. 3, pp. 606–619, 2013.

[9] A. S. Go, D. Mozaffarian, V. L. Roger, E. J. Benjamin, J. D. Berry, M. J. Blaha, S. Dai, E. S. Ford, C. S. Fox, S. Franco, H. J. Fullerton, C. Gillespie, S. M. Hailpern, J. A. Heit, V. J. Howard, M. D. Huffman, S. E. Judd, B. M. Kissela, S. J. Kittner, D. T. Lackland, J. H. Lichtman, L. D. Lisabeth, R. H. Mackey, D. J. Magid, G. M. Marcus, A. Marelli, D. B. Matchar, D. K. McGuire, E. R. Mohler, C. S. Moy, M. E. Mussolino, R. W. Neumar, G. Nichol, D. K. Pandey, N. P. Paynter, M. J. Reeves, P. D. Sorlie, J. Stein, A. Towfighi, T. N. Turan, S. S. Virani, N. D. Wong, D. Woo, and M. B. Turner, "Heart Disease and Stroke Statistics - 2014 Update: A report from the American Heart Association," *Circulation*, vol. 129, no. 3, pp. e29–e166, 2014.

[10] P. Ponikowski, A. Voors, S. Anker, H. Bueno, J. G. F. Cleland, A. Coats, V. Falk, P. v. d. M. T. N. Jose Ramon Gonzale rissis (Greece), Burkert Pieske (Germany), Jillian P. Riley (UK), Giuseppe M. C. Rosano (UK/Italy), Luis M. Ruilope (Spain), Frank Ruschitzka (Switzerland), Frans H. Rutten (The Netherlands), and Document, "2016 ESC Guidelines for the diagnosis and treatment of acute and chronic heart failure," *European Society of Cardiology*, vol. 18, no. 8, pp. 891–975, 2016.

[11] J. Butler, G. C. Fonarow, M. R. Zile, C. S. Lam, L. Roessig, E. B. Schelbert, S. J. Shah, A. Ahmed, R. O. Bonow, J. G. F. Cleland, R. J. Cody, O. Chioncel, S. P. Collins, P. Dunnmon, G. Filippatos, M. P. Lefkowitz, C. N. Marti, J. J. Mcmurray, F. Misselwitz, S. Nodari, C. O. Connor, M. A. Pfeffer, B. Pieske, B. Pitt, G. Rosano, H. N. Sabbah, M. Senni, S. D. Solomon, N. Stockbridge, J. R. Teerlink, V. V. Georgiopoulou, M. Gheorghiade, L. Angeles, S. Francisco, and S. Carolina, "Developing Therapies for Heart Failure With Preserved Ejection Fraction Current State and Future Directions," *JACC: Heart Faulure*, vol. 2, no. 2, pp. 97—-112, 2014.

[12] E. Platz, P. S. Jhund, B. L. Claggett, M. A. Pfeffer, K. Swedberg, C. B. Granger, S. Yusuf, S. D. Solomon, and J. J. Mcmurray, "Prevalence and prognostic importance of precipitating factors leading to heart failure hospitalization : recurrent hospitalizations and mortality," *European Journal of Heart Failure*, vol. 20, pp. 295–303, 2018.

[13] D. A. Kass, "Cardiac resynchronization therapy," *Journal of Cardiovascular Electrophysiology*, vol. 16, no. SUPPL. 1, pp. 35–41, 2005.

[14] D. Durrer, R. T. van Dam, G. E. Freud, M. J. Janse, F. L. Meijler, and R. C. Arzbaecher, "Total excitation of the isolated human heart." *Circulation*, vol. 41, no. 6, pp. 899–912, 1970.

[15] N. Risum, D. Strauss, P. Sogaard, Z. Loring, T. F. Hansen, N. E. Bruun, G. Wagner, and J. Kisslo, "Left bundle-branch block: The relationship between electrocardiogram electrical activation and echocardiography mechanical contraction," *American Heart Journal*, vol. 166, no. 2, pp. 340–348, 2013.

[16] B. Tayal, P. Sogaard, and N. Risum, "Why Dyssynchrony Matters in Heart Failure?" *Cardiac Electrophysiology Clinics*, vol. 11, no. 1, pp. 39–47, 2019.

[17] D. G. Strauss, R. H. Selvester, and G. S. Wagner, "Defining left bundle branch block in the era of cardiac resynchronization therapy," *American Journal of Cardiology*, vol. 107, no. 6, pp. 927–934, 2011.

[18] S. Baldasseroni, C. Opasich, M. Gorini, D. Lucci, N. Marchionni, M. Marini, C. Campana, G. Perini, A. Deorsola, G. Masotti, L. Tavazzi, and A. P. Maggioni, "Left bundle-branch block is associated with increased 1-year sudden and total mortality rate in 5517 outpatients with congestive heart failure: A report from the Italian Network on congestive heart failure," *American Heart Journal*, vol. 143, no. 3, pp. 398–405, 2002.

[19] A. M. Russo, R. F. Stainback, S. R. Bailey, A. E. Epstein, P. A. Heidenreich, M. Jessup, S. Kapa, M. S. Kremers, B. D. Lindsay, L. W. Stevenson, M. B. Alexander, U. Birgersdotter-Green, A. S. Brown, R. A. Grimm, P. J. Hauptman, S. A. Hunt, R. Lampert, J. Lindenfeld, D. J. Malenka, K. Mani, J. E. Marine, E. T. Martin, R. L. Page, M. W. Rich, P. D. Varosy, M. N. Walsh, M. J. Wolk, J. U. Doherty, P. S. Douglas, R. C. Hendel, C. M. Kramer, J. K. Min, M. R. Patel, L. Shaw, and J. M. Allen, "ACCF/HRS/AHA/ASE/HFSA/SCAI/SCCT/SCMR 2013 appropriate use criteria for implantable cardioverter-defibrillators and cardiac resynchronization therapy," *Journal of the American College of Cardiology*, vol. 61, no. 12, pp. 1318–1368, 2013.

[20] G. B. Bleeker, M. J. Schalij, S. G. Molhoek, H. F. Verwey, E. R. Holman, and J. J. Bax, "Relationship between QRS duration and left ventricular dyssynchrony in patients with end-stage heart failure." *Journal of cardiovascular electrophysiology*, vol. 15, no. 5, pp. 544–549, 2004.

[21] E. S. Chung, A. R. Leon, L. Tavazzi, J. P. Sun, P. Nihoyannopoulos, J. Merlino, W. T. Abraham, S. Ghio, C. Leclercq, J. J. Bax, C. M. Yu, J. Gorcsan, M. S. J. Sutton, J. D. Sutter, and J. Murillo, "Results of the predictors of response to crt (prospect) trial," *Circulation*, vol. 117, no. 20, pp. 2608–2616, 2008.

[22] E. Bertaglia, F. Migliore, A. Baritussio, A. De Simone, A. Reggiani, D. Pecora, A. D'Onofrio, A. Rapacciuolo, G. Savarese, A. Pierantozzi, B. Marenna, F. Ruffa, M. Campari, M. Malacrida, and G. Stabile, "Stricter criteria for left bundle branch block diagnosis do not improve response to CRT," *PACE - Pacing and Clinical Electrophysiology*, vol. 40, no. 7, pp. 850–856, 2017.

[23] N. Risum, B. Tayal, T. F. Hansen, N. E. Bruun, M. T. Jensen, T. K. Lauridsen, S. Saba, J. Kisslo, J. Gorcsan, and P. Sogaard, "Identification of

Typical Left Bundle Branch Block Contraction by Strain Echocardiography Is Additive to Electrocardiography in Prediction of Long-Term Outcome after Cardiac Resynchronization Therapy," *Journal of the American College of Cardiology*, vol. 66, no. 6, pp. 631–641, 2015.

[24] C. Ypenburg, J. J. Westenberg, G. B. Bleeker, N. V. de Veire, N. A. Marsan, M. M. Henneman, E. E. van der Wall, M. J. Schalij, T. P. Abraham, S. S. Barold, and J. J. Bax, "Noninvasive Imaging in Cardiac Resynchronization Therapy-Part 1: Selection of Patients," *Pace-Pacing and Clinical Electrophysiology*, vol. 31, no. 11, pp. 1475–1499, 2008.

[25] M. Jastrzębski, P. Kukla, R. Kisiel, K. Fijorek, P. Moskal, and D. Czarnecka, "Comparison of four LBBB definitions for predicting mortality in patients receiving cardiac resynchronization therapy," *Annals of Noninvasive Electrocardiology*, vol. 23, no. 5, pp. 1–10, 2018.

[26] R. M. Lang, L. P. Badano, V. Mor-Avi, J. Afilalo, A. Armstrong, L. Ernande, F. A. Flachskampf, E. Foster, S. A. Goldstein, T. Kuznetsova, P. Lancellotti, D. Muraru, M. H. Picard, E. R. Rietzschel, L. Rudski, K. T. Spencer, W. Tsang, and J. U. Voigt, "Recommendations for cardiac chamber quantification by echocardiography in adults: An update from the American society of echocardiography and the European association of cardiovascular imaging," *European Heart Journal Cardiovascular Imaging*, vol. 16, no. 3, pp. 233–271, 2015.

[27] H. Dalen, A. Thorstensen, L. J. Vatten, S. A. Aase, and A. Stoylen, "Reference values and distribution of conventional echocardiographic Doppler measures and longitudinal tissue Doppler velocities in a population free from cardiovascular disease," *Circulation: Cardiovascular Imaging*, vol. 3, no. 5, pp. 614–622, 2010.

[28] B. H. Amundsen, T. Helle-Valle, T. Edvardsen, H. Torp, J. Crosby, E. Lyseggen, A. Støylen, H. Ihlen, J. A. Lima, O. A. Smiseth, and S. A. Slørdahl, "Noninvasive myocardial strain measurement by speckle tracking echocardiography: Validation against sonomicrometry and tagged magnetic resonance imaging," *Journal of the American College of Cardiology*, vol. 47, no. 4, pp. 789–793, 2006. [Online]. Available: http://dx.doi.org/10.1016/j.jacc.2005.10.040

[29] C. M. Tracy, A. E. Epstein, D. Darbar, J. P. DiMarco, S. B. Dunbar, N. M. Estes, T. B. Ferguson, S. C. Hammill, P. E. Karasik, M. S. Link, J. E. Marine, M. H. Schoenfeld, A. J. Shanker, M. J. Silka, L. W. Stevenson, W. G. Stevenson, and P. D. Varosy, "2012 ACCF/AHA/HRS Focused Update of the 2008 Guidelines for Device-Based Therapy of Cardiac Rhythm Abnormalities," *Circulation*, vol. 126, no. 14, pp. 1784–1800, 2012.

[30] L. Verreault-Julien, F. Philippon, É. Charbonneau, D. Kalavrouziotis, É. LeRoux, J.-F. Sarrazin, M. Dubois, P. Voisine, and M. Sénéchal, "Usefulness of cardiac resynchronization therapy in the recovery of patients with left ventricular assist devices," *International Journal of Cardiology*, vol. 223, pp. 297–298, 2016.

[31] P. van der Bijl, M. Khidir, M. Leung, B. Mertens, N. Ajmone Marsan, V. Delgado, and J. J. Bax, "Impact of QRS complex duration and morphology on left ventricular reverse remodelling and left ventricular function improvement after cardiac resynchronization therapy," *European Journal of Heart Failure*, vol. 19, no. 9, pp. 1145–1151, 2017.

[32] B. Brekke, L. C. L. Nilsen, J. Lund, H. Torp, T. Bjastad, B. H. Amundsen, A. Stoylen, and S. a. Aase, "Ultra-high frame rate tissue Doppler imaging," *Ultrasound in medicine & biology*, vol. 40, no. 1, pp. 222–31, 2014.

[33] T. L. Szabo, *diagnostic ultrasound imaging: inside out*, 2nd ed., E. Inc., Ed. Academic Press, 2014.

[34] C. B. Burckhardt, "Speckle in Ultrasound B -Mode Scans," *IEEE Transactions on Sonics and Ultrasonics*, vol. SU-25, no. 1, pp. 1–6, 1978.

[35] C. Moore, J. Castellucci, M. V. Andersen, M. Lefevre, K. Arges, J. Kisslo, and O. T. Von Ramm, "Live high-frame-rate echocardiography," *IEEE Transactions on Ultrasonics, Ferroelectrics, and Frequency Control*, vol. 62, no. 10, pp. 1779–1787, 2015.

[36] L. Tong, A. Ramalli, P. Tortoli, G. Fradella, S. Caciolli, J. Luo, and J. D'hooge, "Wide-angle tissue doppler imaging at high frame rate using multi-line transmit beamforming: An experimental validation In Vivo," *IEEE Transactions on Medical Imaging*, vol. 35, no. 2, pp. 521–528, 2016.

[37] L. Tong, A. Ramalli, R. Jasaityte, P. Tortoli, and J. D'Hooge, "Multi-transmit beam forming for fast cardiac imaging-experimental validation and in vivo application," *IEEE Transactions on Medical Imaging*, vol. 33, no. 6, pp. 1205–1219, 2014.

[38] D. P. Shattuck, M. D. Weinshenker, S. W. Smith, and O. T. von Ramm, "Explososcan: a parallel processing technique for high speed ultrasound imaging with linear phased arrays." *The Journal of the Acoustical Society of America*, vol. 75, no. 4, pp. 1273–1282, 1984.

[39] M. Tanter and M. Fink, "Ultrafast imaging in biomedical ultrasound," *IEEE Transactions on Ultrasonics, Ferroelectrics, and Frequency Control*, vol. 61, no. 1, pp. 102–119, 2014.

[40] A. Ramalli, A. Dallai, E. Boni, L. Bassi, V. Meacci, M. Giovannetti, L. Tong, J. D'Hooge, and P. Tortoli, "Multi transmit beams for fast cardiac imaging towards clinical routine," *IEEE International Ultrasonics Symposium, IUS*, vol. 2016-Novem, no. 324257, pp. 1–4, 2016.

[41] G. Matrone, A. Ramalli, A. S. Savoia, P. Tortoli, and G. Magenes, "High frame-rate, high resolution ultrasound imaging with multi-line transmission and filtered-delay multiply and sum beamforming," *IEEE Transactions on Medical Imaging*, vol. 36, no. 2, pp. 478–486, 2017.

[42] H. Hasegawa and H. Kanai, "High-frame-rate echocardiography using diverging transmit beams and parallel receive beamforming," *Journal of Medical Ultrasonics*, vol. 38, no. 3, pp. 129–140, 2011.

[43] M. Correia, J. Provost, S. Chatelin, O. Villemain, M. Tanter, and M. Pernot, "Ultrafast Harmonic Coherent Compound (UHCC) Imaging for High Frame Rate Echocardiography and Shear-Wave Elastography," *IEEE Transactions on Ultrasonics, Ferroelectrics, and Frequency Control*, vol. 63, no. 3, pp. 420–431, 2016.

[44] P. Hollender, L. Kuo, V. Chen, S. Eyerly, P. Wolf, and G. Trahey, "Scanned 3-D Intracardiac ARFI and SWEI for Imaging Radio-Frequency Ablation Lesions," *IEEE Transactions on Ultrasonics, Ferroelectrics, and Frequency Control*, vol. 64, no. 7, pp. 1034–1044, 2017.

[45] L. Melki, A. Costet, and E. E. Konofagou, "Reproducibility and Angle Independence of Electromechanical Wave Imaging for the Measurement of Electromechanical Activation during Sinus Rhythm in Healthy Humans," *Ultrasound in Medicine and Biology*, vol. 43, no. 10, pp. 2256–2268, 2017.

[46] M. Strachinaru, J. G. Bosch, B. M. van Dalen, L. van Gils, A. F. van der Steen, N. de Jong, M. L. Geleijnse, and H. J. Vos, "Cardiac Shear Wave Elastography Using a Clinical Ultrasound System," *Ultrasound in Medicine and Biology*, vol. 43, no. 8, pp. 1596–1606, 2017.

[47] C. Pislaru, P. A. Pellikka, and S. V. Pislaru, "Wave propagation of myocardial stretch: Correlation with myocardial stiffness," *Basic Research in Cardiology*, vol. 109, no. 6, pp. 1–12, 2014.

[48] H. J. Vos, B. M. van Dalen, I. Heinonen, J. G. Bosch, O. Sorop, D. J. Duncker, A. F. van der Steen, and N. de Jong, "Cardiac Shear Wave Velocity Detection in the Porcine Heart," *Ultrasound in Medicine and Biology*, vol. 43, no. 4, pp. 753–764, 2017.

[49] E. Bunting, C. Papadacci, E. Wan, V. Sayseng, J. Grondin, and E. Konofagou, "Cardiac Lesion Mapping in vivo using Intracardiac Myocardial Elastography," *IEEE Transactions on Ultrasonics, Ferroelectrics, and Frequency Control*, vol. 3010, no. c, pp. 1–1, 2017.

[50] E. Bunting, L. Lambrakos, P. Kemper, W. Whang, H. Garan, and E. Konofagou, "Imaging the Propagation of the Electromechanical Wave in Heart Failure Patients with Cardiac Resynchronization Therapy," *Pacing and Clinical Electrophysiology*, vol. 40, no. 1, pp. 35–45, 2017.

[51] O. Villemain, M. Correia, E. Mousseaux, J. Baranger, S. Zarka, I. Podetti, G. Soulat, T. Damy, A. Hagège, M. Tanter, M. Pernot, and E. Messas, "Myocardial Stiffness Evaluation Using Noninvasive Shear Wave Imaging in Healthy and Hypertrophic Cardiomyopathic Adults," *JACC: Cardiovascular Imaging*, vol. C, pp. 1–11, 2018.

[52] H. Kanai, "Propagation of spontaneously actuated pulsive vibration in human heart wall and in vivo viscoelasticity estimation." *IEEE transactions on ultrasonics, ferroelectrics, and frequency control*, vol. 52, no. 11, pp. 1931–1942, 2005.

[53] ——, "Propagation of Vibration Caused by Electrical Excitation in the Normal Human Heart," *Ultrasound in Medicine and Biology*, vol. 35, no. 6, pp. 936–948, 2009.

[54] J. Doherty, G. Trahey, K. Nightingale, and M. Palmeri, "Acoustic radiation force elasticity imaging in diagnostic ultrasound," *IEEE transactions on ultrasonics, ferroelectrics, and frequency control*, vol. 60, no. 4, pp. 685–701, 2013.

[55] M. L. Palmeri and K. R. Nightingale, "Acoustic radiation force-based elasticity imaging methods," *Interface Focus*, vol. 1, no. 4, pp. 553–564, 2011.

[56] C. Pislaru, M. M. Alashry, J. J. Thaden, P. A. Pellikka, M. Enriquez-Sarano, and S. V. Pislaru, "Intrinsic Wave Propagation of Myocardial Stretch, A New Tool to Evaluate Myocardial Stiffness: A Pilot Study in Patients with Aortic Stenosis and Mitral Regurgitation," *Journal of the American Society of Echocardiography*, vol. 30, no. 11, pp. 1070–1080, 2017.

[57] M. Alessandrini, M. De Craene, O. Bernard, S. Giffard-Roisin, P. Allain, I. Waechter-Stehle, J. Weese, E. Saloux, H. Delingette, M. Sermesant, and J. D'hooge, "A Pipeline for the Generation of Realistic 3D Synthetic Echocardiographic Sequences: Methodology and Open-Access Database," *IEEE Transactions on Medical Imaging*, vol. 34, no. 7, pp. 1436–1451, 2015.

[58] M. De Craene, M. Alessandrini, P. Allain, S. Marchesseau, I. Waechter-Stehle, J. Weese, E. Saloux, H. G. Morales, R. Cuingnet, H. Delingette, M. Sermesant, O. Bernard, and J. D'hooge, "Generation of ultra-realistic synthetic echocardiographic sequences," *2014 IEEE 11th International Symposium on Biomedical Imaging (ISBI)*, pp. 73–76, 2014.

[59] M. Alessandrini, B. Heyde, S. Queirós, S. Cygan, M. Zontak, O. Somphone, O. Bernard, M. Sermesant, H. Delingette, D. Barbosa, M. D. Craene, M. O'Donnell, and J. D'hooge, "Detailed Evaluation of Five 3D Speckle Tracking Algorithms using Synthetic Echocardiographic Recordings," *IEEE Transactions on Medical Imaging*, vol. 35, no. 8, pp. 1915–1926, 2016.

[60] Y. Zhou, S. Giffard-Roisin, M. De Craene, S. Camarasu-Pop, J. D'Hooge, M. Alessandrini, D. Friboulet, M. Sermesant, and O. Bernard, "A Framework for the Generation of Realistic Synthetic Cardiac Ultrasound and Magnetic Resonance Imaging Sequences from the Same Virtual Patients," *IEEE Transactions on Medical Imaging*, vol. 37, no. 3, pp. 741–754, 2018.

[61] T. P. Abraham, V. L. Dimaano, and H.-Y. Liang, "Role of Tissue Doppler and Strain Echocardiography in Current Clinical Practice," *Circulation*, vol. 116, no. 22, pp. 2597–2609, 2007.

[62] E. E. Konofagou, J. Luo, D. Saluja, D. O. Cervantes, J. Coromilas, and K. Fujikura, "Noninvasive electromechanical wave imaging and conduction-relevant velocity estimation in vivo." *Ultrasonics*, vol. 50, no. 2, pp. 208–215, 2010.

[63] A. Costet, E. Wan, E. Bunting, J. Grondin, H. Garan, and E. Konofagou, "Electromechanical wave imaging (EWI) validation in all four cardiac chambers with 3D electroanatomic mapping in canines in vivo," *Physics in Medicine & Biology*, vol. 61, no. 22, pp. 8105 – 8116, 2016.

[64] H. Li, J. Porée, M. H. Roy Cardinal, and G. Cloutier, "Two-dimensional affine model-based estimators for principal strain vascular ultrasound elastography with compound plane wave and transverse oscillation beamforming," *Ultrasonics*, vol. 91, no. April 2018, pp. 77–91, 2019.

[65] M. Correia, I. Podetti, O. Villemain, J. Baranger, M. Tanter, and M. Pernot, "Non-invasive Myocardial Shear Wave Elastography Device for Clinical Applications in Cardiology," *Irbm*, vol. 38, no. 6, pp. 357–362, 2017.

[66] J. Poree, D. Posada, A. Hodzic, F. Tournoux, G. Cloutier, and D. Garcia, "High-Frame-Rate Echocardiography Using Coherent Compounding with Doppler-Based Motion-Compensation," *IEEE Transactions on Medical Imaging*, vol. 35, no. 7, pp. 1647–1657, 2016.

[67] P. Joos, J. Porée, H. Liebgott, D. Vray, M. Baudet, J. Faurie, F. Tournoux, G. Cloutier, B. Nicolas, and D. Garcia, "High-Frame-Rate Speckle-Tracking Echocardiography," *IEEE Trans Ultrason Ferroelectr Freq Control*, vol. 65, no. 5, pp. 720–728, 2018.

[68] P. Song, H. Zhao, M. Urban, A. Manduca, S. Pislaru, R. Kinnick, C. Pislaru, J. Greenleaf, and S. Chen, "Improved Shear Wave Motion Detection Using Pulse-Inversion Harmonic Imaging with a Phased Array Transducer." *IEEE transactions on medical imaging*, vol. 32, no. 12, pp. 2299–2310, 2013.

[69] J. Grondin, V. Sayseng, and E. E. Konofagou, "Cardiac Strain Imaging with Coherent Compounding of Diverging Waves," *IEEE Transactions on Ultrasonics, Ferroelectrics, and Frequency Control*, vol. 3010, no. c, pp. 1–1, 2017.

[70] P. Santos, A. Petrescu, J. Pedrosa, M. Orlowska, V. Komini, J. U. Voigt, and J. D'hooge, "Natural shear wave imaging in the human heart: normal values, feasibility and reproducibility," *IEEE Transactions on Ultrasonics, Ferroelectrics, and Frequency Control*, vol. 66, no. 3, pp. 442–452, 2019.

[71] M. Kornbluth, D. H. Liang, A. Paloma, and I. Schnittger, "Native tissue harmonic imaging improves endocardial border definition and visualization of cardiac structures," *Journal of the American Society of Echocardiography*, vol. 11, no. 7, pp. 693–701, 1998.

[72] K. T. Spencer, J. Bednarz, P. G. Rafter, C. Korcarz, and R. M. Lang, "Use of harmonic imaging without echocardiographic contrast to improve two-dimensional image quality," *American Journal of Cardiology*, vol. 82, no. 6, pp. 794–799, 1998.

[73] E. Cherin, J. K. Poulsen, A. F. Van der Steen, and F. S. Foster, "Comparison of nonlinear and linear imaging techniques at high frequency," *Proceedings of the IEEE Ultrasonics Symposium*, vol. 2, pp. 1639–1644, 2000.

[74] J. Luo and E. Konofagou, "A fast normalized cross-correlation calculation method for motion estimation," *IEEE transactions on ultrasonics, ferroelectrics, and frequency control*, vol. 57, no. 6, pp. 1347–57, 2010.

[75] J. Provost, W.-N. Lee, K. Fujikura, and E. E. Konofagou, "Electromechanical Wave Imaging of Normal and Ischemic Hearts In Vivo," *IEEE Transactions on Medical Imaging*, vol. 29, no. 3, pp. 625–635, 2010.

[76] J. Provost, A. Costet, E. Wan, A. Gambhir, W. Whang, H. Garan, and E. E. Konofagou, "Assessing the atrial electromechanical coupling during atrial focal tachycardia, flutter, and fibrillation using electromechanical wave imaging in humans," *Computers in Biology and Medicine*, vol. 65, pp. 161–167, 2015.

[77] M. V. Andersen, C. Moore, K. Arges, P. Søgaard, L. R. Østergaard, S. E. Schmidt, J. Kisslo, and O. T. Von Ramm, "High-Frame-Rate Deformation Imaging in Two Dimensions Using Continuous Speckle-Feature Tracking," *Ultrasound in Medicine and Biology*, vol. 42, no. 11, pp. 2606–2615, 2016.

[78] M. V. Andersen, C. Moore, S. E. Schmidt, P. Søgaard, J. J. Struijk, J. Kisslo, and O. T. V. Ramm, "Feature Tracking Algorithm for Circumferential Strain using High Frame Rate Echocardiography," in *Computing in Cardiology Conference (CinC), 2016*, vol. 43, 2016, pp. 885–888.

[79] M. V. Andersen, C. Moore, P. Søgaard, D. Friedman, B. D. Atwater, K. Arges, M. LeFevre, J. J. Struijk, J. Kisslo, S. E. Schmidt, and O. T. von Ramm, "Quantitative Parameters of High-Frame-Rate Strain in Patients with Echocardiographically Normal Function," *Ultrasound in Medicine and Biology*, vol. Article in, no. 00, pp. 1–11, 2019.

[80] M. S. Andersen, C. Moore, M. LeFevre, K. Arges, D. J. Friedman, B. D. Atwater, J. Kisslo, P. Søgaard, J. J. Struijk, O. T. von Ramm, and S. E. Schmidt, "Contractile Fronts In The Interventricular Septum: A Case For High Frame Rate Echocardiographic Imaging," *Ultrasound in Medicine & Biology (IN REVIEW)*, vol. 0, no. 0, pp. 1–10, 2019.

[81] R. H. Helm, C. Leclercq, O. P. Paris, C. Ozturk, E. McVeigh, A. C. Lardo, and D. A. Kass, "Cardiac dyssynchrony analysis using circumferential versus longitudinal strain: Implications for assessing cardiac resynchronization," *Circulation*, vol. 111, no. 21, pp. 2760–2767, 2005.

[82] V. Delgado, C. Ypenburg, R. J. van Bommel, L. F. Tops, S. a. Mollema, N. A. Marsan, G. B. Bleeker, M. J. Schalij, and J. J. Bax, "Assessment of Left Ventricular Dyssynchrony by Speckle Tracking Strain Imaging," *Journal of the American College of Cardiology*, vol. 51, no. 20, pp. 1944–1952, 2008.

[83] C. Zhang and Z. Zhang, "2D Ultrasonic Elastography Using Beam Steering and Iterative Correction," *Journal of Medical Imaging and Health Informatics*, vol. 7, no. 1, pp. 211 —- 216, 2017.

[84] V. Sayseng, J. Grondin, and E. E. Konofagou, "Optimization of Transmit Parameters in Cardiac Strain Imaging with Full and Partial Aperture Coherent Compounding," *IEEE Transactions on Ultrasonics, Ferroelectrics, and Frequency Control*, vol. 65, no. 5, pp. 684–696, 2018.

[85] E. Bunting, J. Provost, and E. Konofagou, "Stochastic precision analysis of two-dimensional cardiac strain estimation in vivo," *Phys Med Biol*, vol. 59, no. 22, pp. 6841 —- 6858, 2014.

[86] S. A. Aase, S. R. Snare, H. Dalen, A. Støylen, F. Orderud, and H. Torp, "Echocardiography without electrocardiogram," *European Journal of Echocardiography*, vol. 12, no. 1, pp. 3–10, 2011.

Part VI

Publications

List of publications

M. V. Andersen, C. Moore, K. Arges, P. Søgaard, L. R. Østergaard, S. E. Schmidt, J. Kisslo, and O. T. Von Ramm, "High-Frame-Rate Deformation Imaging in Two Dimensions Using Continuous Speckle-Feature Tracking," *Ultrasound in Medicine and Biology*, vol. 42, no. 11, pp. 2606–2615, 2016.

M. V. Andersen, C. Moore, S. E. Schmidt, P. Søgaard, J. J. Struijk, J. Kisslo, and O. T. V. Ramm, "Feature Tracking Algorithm for Circumferential Strain using High Frame Rate Echocardiography," in *Computing in Cardiology Conference (CinC), 2016*, vol. 43, 2016, pp. 885–888.

M. V. Andersen, C. Moore, P. Søgaard, D. Friedman, B. D. Atwater, K. Arges, M. LeFevre, J. J. Struijk, J. Kisslo, S. E. Schmidt, and O. T. von Ramm, "Quantitative Parameters of High-Frame-Rate Strain in Patients with Echocardiographically Normal Function," *Ultrasound in Medicine and Biology*, vol. Article in, no. 00, pp. 1–11, 2019.

M. S. Andersen, C. Moore, M. LeFevre, K. Arges, D. J. Friedman, B. D. Atwater, J. Kisslo, P. Søgaard, J. J. Struijk, O. T. von Ramm, and S. E. Schmidt, "Contractile Fronts In The Interventricular Septum: A Case For High Frame Rate Echocardiographic Imaging," *Ultrasound in Medicine & Biology (IN REVIEW)*, vol. 0, no. 0, pp. 1–10, 2019.

Study A

High-Frame-Rate Deformation Imaging in Two Dimensions Using Continuous Speckle-Feature Tracking

Martin V. Andersen, Cooper Moore, Kristine Arges, Peter Søgaard, Lasse R. Østergaard, Samuel E. Schmidt , Joseph Kissloand Olaf T. von Ramm

The paper has been published in the
Journal or Ultrasound in Medicine and Biology Vol. 42(11), pp. 2606–2615, 2016.

The layout has been revised.

Study B

Feature tracking algorithm for circumferential strain using high frame rate echocardiography

Martin V. Andersen, Cooper Moore, Samuel E. Schmidt, Peter Søgaard, Johannes J. Struijk, Joseph Kisslo, and Olaf T. von Ramm

The paper was published in
Computing in Cardiology Vol. 43, pp. 885–888, 2016.

Study C

Quantitative Parameters of High-Frame-Rate Strain in Patients with Echocardiographically Normal Function

Martin V. Andersen, Cooper Moore, Peter Søgaard, Daniel Friedman, Brett D. Atwater, Kristine Arges, Melissa LeFevre, Johannes J. Struijk, Joseph Kisslo, Samuel E. Schmidt, and Olaf T. von Ramm

Paper in press
Journal or Ultrasound in Medicine and Biology Vol. 45(5), pp. 1197–1207, 2019.

The layout has been revised.

Study D

Contractile Fronts In The Interventricular Septum: A Case For High Frame Rate Echocardiographic Imaging

Martin S Andersen, Cooper Moore, Melissa LeFevre, Kristine Arges, Daniel J Friedman, Brett D Atwater, Joseph Kisslo, Peter Søgaard, Johannes J Struijk, Olaf T von Ramm, and Samuel E Schmidt

The paper is under review in
Ultrasound in Medicine & Biology Vol. 0(0), pp. 1–10, 2019.

The layout has been revised.

ISSN (online): 2246-1302
ISBN (online): 978-87-7210-476-8

AALBORG UNIVERSITY PRESS